THE EFFECTS OF DENSITY ON BURNING RATES OF AP/HTPB COMPOSITE SOLID PROPELLANTS

A Thesis

By

ALVIN HONG

Submitted to the Graduate and Professional School of
Texas A&M University
In partial fulfillment of the requirements for the degree of

MASTER OF SCIENCE

Chair of Committee,	Eric L. Petersen
Committee Members,	Timothy Jacobs
	Adonios Karpetis
Head of Department,	Bryan Rassmussen

May 2022

Major Subject: Mechanical Engineering

ABSTRACT

Within identical composite solid AP/HTPB propellant formulations, the densities of each individual propellant can greatly vary depending on their manufacturing quality. Propellants with lower densities than their theoretical maximum densities usually indicate the presence of air bubbles, or voids, within the propellant structure. The effects of these voids on the burning rates of propellants were investigated and thoroughly characterized by comparing the manufacturing quality and performance of propellants with differing densities. Baseline AP/HTPB propellants were manufactured using a custom designed extruder that can produce high density propellants. This custom extruder can also be modified to create low density propellants by deliberately introducing air into the system to induce the formation of voids. A burning rate curve for low-, medium-, and high-density propellants was developed for a pressure range between 500 and 2500 psia. These results indicate that low-density propellants will have measurably higher burning rates than high-density propellants. Numerous propellants were also repeatedly tested for burning rates at 500 and at 3000 psia to determine how the scatter and deviation of burning rates are affected by propellant density at both low and high pressures. These results indicate that low-density propellants will display a higher burning rate variance compared to high-density propellants. In addition, the low-density propellants were shown to have statistically significant different burning rates compared to the high-density propellants at low pressures. This study demonstrates that voids in propellant can greatly impact the performance and safety of a rocket motor.

DEDICATION

I would like to thank Dr. Eric Petersen who provided me with the opportunity to be a part of the incredible research being conducted in his lab. I would also like to thank Dr. Timothy Jacobs and Dr. Adonios Karpetis for taking the time to be a part of my committee.

I would like to thank my current and former colleagues that I had the pleasure of working with in the Petersen Research Group: Dr. Catherine Dillier, Dr. James Thomas, Felix Rodriguez, David Teitge, Kristen Herder, and Thomas Sammet. I would also like to thank Dr. David Reid and the Helicon Chemical Company for letting me be a part of their research.

Lastly, I would like to thank my family and friends who have supported me and pushed me to become more than I thought I could be.

ACKNOWLEDGMENTS

This research was supported by service project funding to the Petersen Research Group and Texas A&M Experiment Station (TEES) Turbomachinery Laboratory.

CONTRIBUTORS AND FUNDING SOURCES

Contributors

This work was supported by a thesis committee consisting of Professor Eric Petersen [advisor] and Professor Timothy Jacobs of the Department of Mechanical Engineering and Professor Adonios Karpetis of the Department of Aerospace Engineering.

The custom propellant extruder was designed with the aid of Thomas Sammet and Kristen Herder and manufactured by Carl Johnson. The Archimedes' method of testing propellant density was designed with the aid of Thomas Sammet and Dr. Catherine Dillier. The burning rate and propellant density data analyzed in Chapter VI was collected with the help of Kristen Herder.

All other work conducted for the thesis was completed by the student independently.

Funding Sources

Graduate study was partially supported by a fellowship from Texas A&M University and a research fellowship from Baker Risk.

NOMENCLATURE

AP	Ammonium Perchlorate
DAQ	Data Acquisition
HTPB	Hydroxyl-Terminated Polybutadiene
IPDI	Isophorone Diisocyanate
RSS	Root-Sum-Square
TMD	Theoretical Maximum Density

TABLE OF CONTENTS

LIST OF FIGURES

LIST OF TABLES

CHAPTER I

INTRODUCTION

Composite Solid Propellants

Composite solid propellants are a class of rocket propellants that commonly serves in the propulsion system for military armaments, spacecraft solid rocket boosters, research sounding rockets, and amateur model rockets. While not as commonly used today for space launch vehicles due to poorer performance compared to modern day liquid propellants, composite solid propellants are still regularly used in military applications within the earth's atmosphere due to their ease of storage and ability to be launched at a moment's notice. Composite solid propellants have the advantage of being much simpler to manufacture, store, and launch compared to liquid propellants. This convenience makes composite solid propellants an attractive option when choosing a propellant for a propulsion system.

The most elementary configuration of a baseline composite solid propellants is formed by combining an oxidizer, a binder, and a curing agent into a viscous, heterogeneous mixture and letting it cure until it becomes a solid. Composite solid propellants can also contain a variety of additives to help improve its overall performance. Metal powdered fuels can be added to improve a propellants energy density, adiabatic flame temperature, and specific impulse [1]. Metal oxide catalysts can be added to either increase or decrease the burning rate of propellants [2]. Additional additives can also be used to tailor the performance, manufacturability, and mechanical properties of composite solid propellants depending on the application.

The composite solid propellants used in this thesis are composed of ammonium perchlorate (AP) as the oxidizer, hydroxyl-terminated polybutadiene (HTPB) as the binder, and isophorone diisocyanate (IPDI) as the curative. Ammonium perchlorate (NH_4ClO_4) was selected

as the oxidizer of choice as it is readily available, has good compatibility with other common propellant chemicals, and provides better performance compared to common alternatives such as ammonium nitrate (NH_4NO_3) and potassium perchlorate ($KClO_4$) [3]. Hydroxyl-terminated polybutadiene was chosen as the hydrocarbon polymer binder as it is readily available, provides good mechanical properties once it is cured, and allows for higher solids loading propellants [3]. Once the AP and HTPB are combined into a heterogeneous mixture, the IPDI curative is added to remove the hydroxyl group from the liquid binder which allows the polymers to form longer chains and solidify [3]. For this thesis, the study was conducted on baseline composite solid propellants and no additional additives were used.

One common method used to modify the performance, manufacturability, and mechanical properties of a composite solid propellant is to alter the AP particle distribution. Particle distribution refers to the number of distinct particle size groups that are used in a composite solid propellant. A propellant consisting of only a single, distinct AP particle size is categorized as a monomodal propellant, while a propellant consisting of two distinct AP particle sizes, a combination of fine/coarse grade AP, is categorized as a bimodal propellant. A propellant consisting of three distinct AP particle sizes, a combination of fine/medium/coarse grade AP, is categorized as a trimodal propellant. Figure 1 depicts a representation of the cross section of a monomodal, bimodal, and trimodal propellant with their respective distributions of different distinct AP particle sizes. Propellants with wider AP particle distributions generally have better manufacturability compared to propellants with narrower AP particle distributions. Wider AP particle distribution improves the particle packing of AP and lowers the mixture viscosity, as the smaller AP particles are able to fill in the crevices created by larger AP particles [4]. Both monomodal and bimodal formulations were used in this study.

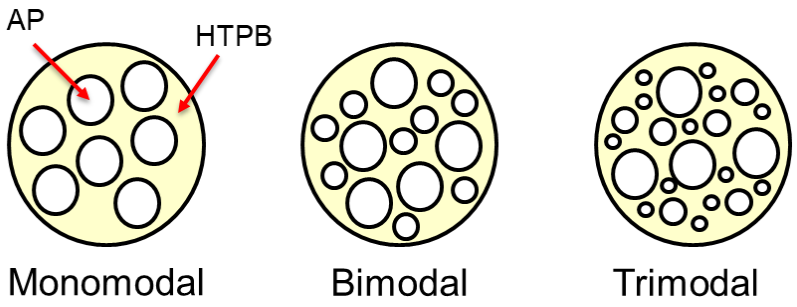

Figure 1. An illustration of the different cross sections of a monomodal, bimodal, and trimodal AP/HTPB propellant. Wider AP particle distributions can improve particle packing as smaller AP particles fill in the crevices in between larger AP particles.

Propellant Burning Rate

One of the most important performance metrics in composite solid propellants is the propellant burning rate. Burning rate is a measure of how much propellant is burned in a certain amount of time [5]. The burning rate equation, also known as Vieille's Law, is in the form of a power law written as:

$$r = aP^n \tag{1}$$

In Eq. 1, the burning rate r is dependent on factors of both propellant composition as well as rocket motor design. The pressure exponent n in Eq. 1 is a function of the propellant composition and is typically a value between 0.3 and 0.6 [6]. Some examples of factors in a propellant's composition that affects its burning rate are oxidizer/fuel content, average particle size, addition of catalysts, sample density, etc. [5]. The combustion chamber pressure P can be affected by the design of a rocket motor and the rate at which hot gases are released from the propellant as it burns. In Eq. 1, a represents the temperature coefficient and is usually a value between 0.002 and 0.05 [5]. The Petersen Research Group at Texas A&M University typically collects propellant burning rate data in a strand burner at pressures between 500 and 5000 psia. However, there is also a second, very-high-pressure strand burner within the facility that is

designed to safely test up to 10,000 psia [7]. Propellant burning rate curves generally take the form of a linear regression line with a positive slope when plotted with respect to pressure on a log-log scale. However, at elevated pressures typically above 3000 psia, most AP-based composite solid propellants will exhibit a sharp increase in burning rate with respect to pressure [6]. This feature is known as an exponent break and can be important when considering rocket motor performance and safety. The exponent break feature begins at a pressure identified as the characteristic pressure, P^*. This sharp increase in burning rate at elevated combustion chamber pressures can improve rocket motor performance by being able to convert more chemical energy into kinetic energy in a shorter amount of time. However, if the rocket motor is not designed to operate at extremely high pressures and forces, a sharp increase in burning rate can be catastrophic to the rocket. Figure 2 shows an example of two different propellant formulations that both display an exponent break feature which begins at the characteristic pressure, P^*. In this thesis, propellants are studied at both low and high pressures to better understand how variations in propellant densities will affect its burning rate in different pressure regions.

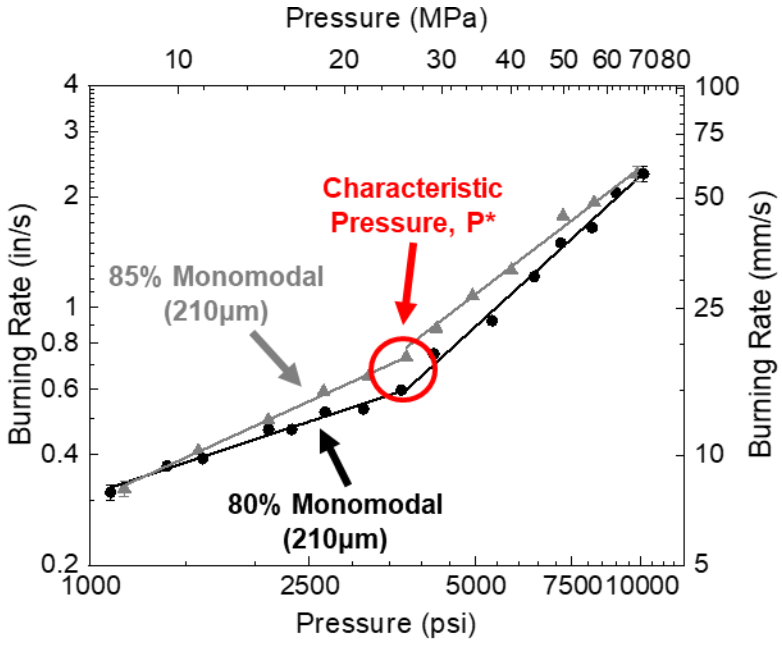

Figure 2. Burning rates curves of two monomodal propellants with different solids loading between 1000 and 10,000 psia. The characteristic pressure, P^*, indicates the beginning of the exponent break feature and occurs somewhere between 3500 and 4000 psia for these two propellants [6].

Burning rate is an important performance metric as it correlates to the amount of thrust and specific impulse a rocket motor can achieve. As the rocket propellant burns, it generates high-pressure and high-temperature gases that expand from the combustion chamber out through a rocket nozzle to produce a thrust force. The general rocket thrust equation is described as:

$$F = \dot{m}v_e + (P_e - P_0)A_e \tag{2}$$

Where $\dot{m}$ is the propellant mass flow rate, v_e is the exit velocity of the hot gases from the rocket nozzle, $(P_e - P_0)$ is pressure differential of the hot gases at the nozzle exit and back pressure conditions, and A_e is the exit area of the rocket nozzle. From Eq. 2, an increase in the propellant mass flow rate will result in an increase of the rocket thrust force. The mass flow rate $\dot{m}$ of the hot gases generated from a burning propellant is given as:

$$\dot{m} = A_b r \rho_b \tag{3}$$

From Eq. 3, an increase in the propellant burning rate r will result in an increase in the mass flow rate of hot gases leaving the rocket nozzle and allow for higher thrust forces to be achieved. An increase in burning rate can also contribute to higher thrust forces by increasing the hot gas exit velocity and exit pressure from Eq. 2. Although, the hot gas exit velocity and exit pressure are also highly dependent on the design of the rocket nozzle itself. The propellant density ρ_b can be increased by improving particle packing so more oxidizer and fuel can be introduced to increase the overall energy density and theoretical maximum density (TMD) of the propellant. However, an increase in solids loading, which is the percentage of solid ingredients compared to liquid ingredients in a propellant mixture, can cause issues when manufacturing composite solid propellants. Figure 3 depicts the cross-sectional area of a propellant with low solids loading compared to one with high solids loading. Increasing the solids loading will increase the viscosity of the propellant mixture. Composite solid propellants, especially those with high solids loading, often do not achieve their TMD due to poor mixing quality and flaws in the propellant grain structure caused by difficulties during the casting or extrusion process [8]. Even identical propellant formulations can have drastically different densities depending on the overall manufacturing quality. This density difference can result in drastic changes in the performance and safety of a solid rocket motor.

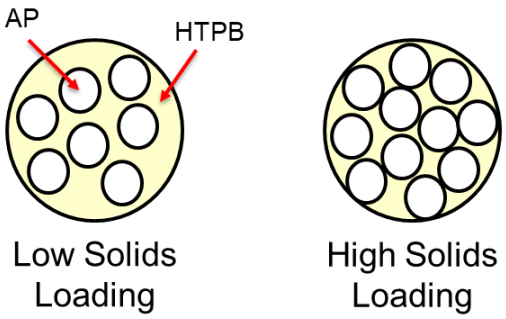

Figure 3. An illustration of the different cross sections of AP/HTPB propellants with low and high solids loading. Higher solids loading propellants can be more difficult to manufacture and result in more defects.

The burning area A_b is an important variable when determining the mass flow rate and thrust profile of a rocket motor which is why propellant grain geometries play a big part in rocket motor design [9]. For large-scale applications, solid rocket motors are generally burned perpendicular from the center, axial direction of the propellant. In the literature however, propellants are usually burned in the axial direction when experimentally determining the burning rates of composite solid propellants. The propellant should burn in a linear fashion for the most precise results. If the propellant burns at an angle, the burning area can constantly alter and cause an unintentional change in propellant burning rate and mass flow rate. Figure 4 depicts a propellant burning in the axial direction in an ideal, linear fashion as well as a propellant that is burning at an angle.

Figure 4. Left: Image of AP/HTPB propellant burning linearly in the axial direction. Right: Image of AP/HTPB propellant burning at an angle in the axial direction.

An increase in rocket thrust force can also result in an increase in specific impulse I_{sp} which is given as:

$$I_{sp} = \frac{I}{mg_0} = \frac{F}{\dot{m}g_0} \tag{4}$$

Specific impulse is one of the most important measurements of efficiency for a rocket propulsion system. A rocket propulsion system with a high specific impulse can utilize the mass of the propellant more efficiently. Since minimizing the overall weight of a rocket allows for a larger payload capacity, a high specific impulse is very desirable when selecting a rocket propulsion system. To increase the specific impulse I_{sp} of a rocket propulsion system, the thrust force F should be maximized while the mass flow rate $\dot{m}$ should be minimized. The variable g_0 is the gravitational acceleration constant and cannot be altered. Increasing the burning rate of a

propellant will increase the thrust force as previously mentioned, but as a result will also increase the mass flow rate which should be minimized for improved specifical impulse. So, it is important to design a propellant formulation with the correct balance of burning rate, mass flow rate, thrust force, and specific impulse for optimal performance.

As previously mentioned, an increase in propellant density will result in a higher mass flow rate and thus, increased thrust force. But when comparing propellant samples from identical formulations, the densities can be drastically different depending on the manufacturing quality. If a propellant is poorly manufactured, it can contain small voids that reduces its overall density. This thesis analyzes how variations in the density of identical propellant formulations will affect the burning rates of baseline composite solid propellants. Characterizing this feature is extremely important when considering the performance and safety of a solid rocket motor.

Thesis Outline

In Chapter II, an in-depth review of available literature on the causes and effects of voids in propellants are discussed. An emphasis is placed on the effects that voids can have on propellant density and burning rate. The propellant formulations that are used this thesis are discussed in Chapter III. This chapter also describes a new mechanical extrusion process that was designed for this thesis. Chapter IV describes the testing procedures that were used to collect measurements on propellant density and burning rate. The results and estimated uncertainties of the experiment are discussed in Chapter V. Lastly, Chapter VI provides a brief summary of the experiment and key findings from the study.

CHAPTER II

BACKGROUND

The performance and safety of a rocket motor can be dictated by the formations of small voids on the interior and surface of a composite solid propellant. Study on the causes of these voids and how they impact the performance of a rocket motor has been an important subject of research for many years. Because voids in propellants can cause catastrophic accidents, great lengths have been taken to improve the propellant manufacturing process to try and mitigate this issue. Methods such as x-ray radiography, magnetic resonance, and ultrasound techniques have also been developed to identify the presence of voids in propellants [10-13]. Figure 5 displays a propellant with easily identifiable exterior and interior voids. Modeling simulations have also been constructed to predict the presence of voids based on different propellant formulations and how these voids will affect the performance and safety of a rocket motor [14]. In the literature, it is well agreed upon that the presence of voids in propellants will decrease propellant density and cause an increase in propellant burning rate [12-18].

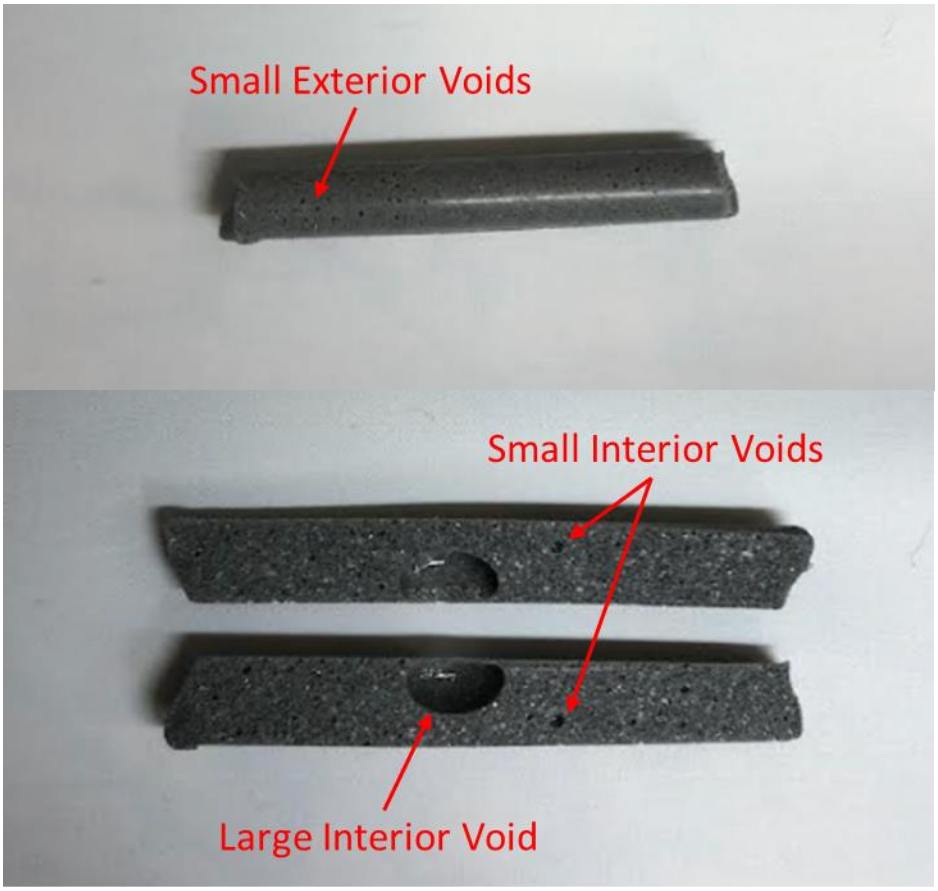

Figure 5. Top: Outside surface of a solid propellant sample with small exterior voids. Bottom: Cross sectional cut of a solid propellant with an extremely large interior void accompanied with additional smaller voids.

A typical AP-based composite propellant is generally accepted to behave under the multiple-flame model while it is burning [19]. This multiple-flame model consists of an AP monopropellant flame located a small distance away from the surface of the AP particle; a premixed flame where the oxidizer and binder decomposition products are thoroughly mixed; and a diffusion flame that follows the previous two flame structures. Voids in propellants are able to increase the burning rate of a propellant through an increase in the propellant burning area and an alteration of the flame structure [18]. An increase in the propellant burning area will

allow for a larger flame front and result in an increase in heat conduction to the unburned propellant and deflagration rate of propellant material. Since the regression rate of the void is larger than both the AP and HTPB, the flame front is brought closer to the propellant burning surface where the voids are located. Bringing the flame front closer to the propellant burning surface causes the temperature at the burning area to increase, which will result in an increase in burning rate. Figure 6 depicts a schematic of how a void in a propellant can increase the burning area and alter the flame structure to increase propellant burning rate.

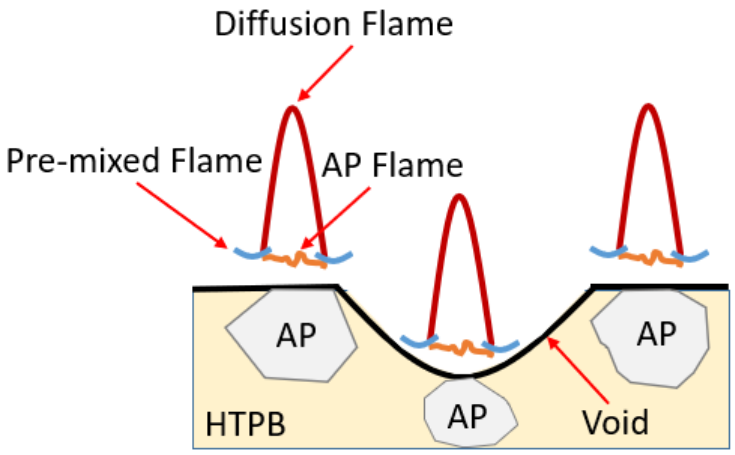

Figure 6. Representation of a void in a propellant and the resultant change in burning area and flame structure.

Voids in propellants are generally assumed to consist of many isolated bubbles containing air or other trapped gases [14]. The presence of voids can often be indicated when a propellant has a density lower than the TMD, as these trapped gases have a much lower density than the ingredients in a composite solid propellant. Table 1 shows the different densities of common chemicals used in composite solid propellants compared to the density of air. These voids can be caused by a variety of factors such as inadequate mixing, defects during propellant

casting/extruding, and chemical reactions between different propellant ingredients during and after the solidification process.

Table 1: Densities of common propellant chemicals compared to propellant air bubbles.

Chemicals	Density at 23°C (g/cm^3)
Hydroxyl-Terminated Polybutadiene (R45M HTPB)	0.901
Ammonium Perchlorate (AP)	1.950
Isophorone Diisocyanate (IPDI)	1.062
Aluminum	2.710
Air	1.225×10^{-3}

In general, the first step in large-scale manufacturing of composite solid propellants is combining the raw propellant ingredients into a vacuum-sealed planetary mixer to create a heterogeneous viscous propellant slurry [20]. This propellant slurry is then cast into a rocket motor casing with a removable mandrel insert that creates the internal propellant grain geometry. This process normally takes plus under vacuum to remove gases and reduce the likelihood of voids forming within the propellant [20]. Afterwards, the rocket motor is placed in an oven where the propellant slurry will cure until it becomes completely solid. This curing process is accelerated while the propellant slurry is under elevated temperatures [21].

Large-scale manufacturing of composite solid propellants requires the use of large industrial mixers to adequately create a homogeneous mixture. If inadequate mixing occurs, there could be an uneven distribution of propellant ingredients which could cause large fluctuations in propellant sample densities. A study conducted by Verma et al. [12] explored the effect of mixer size on the density and burning rate of composite solid propellants. The mixer

sizes used in their study had capacities of 15, 70, 200, and 1000 g. It was determined that a decrease in mixer capacity resulted in a decrease in propellant density. These propellant samples were then tested for burning rate where a decrease in mixer capacity, and thus propellant density, resulted in an increase in burning rate. However, the propellant samples that were discovered to contain voids were discarded and were not tested for burning rate. So, the effect that their mixer size had on the formation of voids and their effect on propellant burning rate was not measured. The authors of this research concluded that the cause of the decrease in propellant density was due to the surface area-to-volume ratio of the mixer blade and mixer. This ratio is larger for smaller-capacity mixers which creates more surface area for the AP to adhere to. The smaller capacity mixers also caused a reduction in the propellant's AP solids loading since it is very difficult to ensure that every single particle of AP is removed from the mixer and cast into the rocket motor casing. This missing AP resulted in a decrease in propellant density even though the propellant formulations were initially identical for all mixer sizes. It was also discovered that a higher concentration of coarse AP particles adhered to the surface of the mixer compared to fine AP particles. This preferential loss of larger AP caused higher amounts of fine AP particles to be present in the propellants with lower densities which resulted in an increase in burning rate.

One common method to mitigate the formation of voids is to perform the mixing and casting process under a vacuum. Mixing while under a vacuum allows for air and other trapped volatiles to be removed from the propellant slurry [14, 17, 22]. During the mixing process, air can be worked into the propellant if the mixing takes place under normal atmospheric conditions. Introducing a vacuum removes air from the process and prevents pockets of air from being trapped in the crevices of the propellant slurry. While combining different chemicals, there is also the possibility of developing chemical reactions that can produce volatiles within the

propellant slurry mixture. For example, if water is unintentionally absorbed by propellant ingredients, it can react with the isophorone diisocyanate curative to produce gaseous carbon dioxide [23]. Additional chemical reactions can potentially produce other volatiles in both gaseous and liquid states. It is much more difficult to remove unwanted liquid volatiles compared to gaseous volatiles as the liquid volatiles are thoroughly incorporated into the propellant slurry. However, the unwanted liquid volatiles can be converted to gaseous products through a vaporization process that is enhanced under vacuum. Materials will vaporize at a lower temperature as their vapor pressure decreases. Mixing under vacuum has the added benefit of being able to remove these volatile gases as well as lowering the temperature at which certain volatile liquids can readily vaporize. If these volatiles are not allowed to be degassed, they can cause numerous 1-to-3 mm diameter voids to be formed in the cured propellant [17].

The Petersen Research Group manufactures composite solid propellants in a small-scale laboratory setting and typically mixes propellants by hand. While not mixed directly under vacuum, the propellant slurries are allowed to degas in a vacuum chamber after mixing in each solid ingredient to remove any potential volatiles that may have formed. This hand-mixing process has been refined over the years and yields comparable burning rate results compared to propellants mixed in large-scale industrial mixers [24].

Once all the propellant ingredients have been thoroughly mixed, the next step is to either cast or extrude the propellant into the desired shape and grain geometry. After the propellant has been cast or extruded, it is placed in an oven where it will cure into a solid. As previously mentioned, casting a propellant involves pouring the propellant slurry into rocket motor casing with a removeable mandrel insert where it will cure into the desired grain geometry. Extruding a propellant involves mechanically pressing the propellant slurry through a die to form its desired

shape and grain geometry. To mitigate void formation, these methods usually occur under a vacuum to remove any entrained air or potential volatiles that could be trapped in the propellant slurry [14]. During these processes, some common manufacturing deficiencies that can be found include voids, cracks, and debonding of propellant material [13, 25]. Debonding can occur from the high internal stresses during the curing process and can lead to crack propagation throughout the propellant [13]. The presence of voids can also aid in crack formation as they provide potential nucleation points and pathways through which the cracks can propagate. Because the cast or extruded propellant can be fragile early into its curing phase, improper handling of the propellant can lead to cracks and other deformities in the propellant structure. Thermal expansion has been discovered as another factor that could cause voids and cracks to form in propellants when curing at elevated temperatures [13].

Voids and cracks in propellants can potentially result in elevated burning rates and uncontrollable explosion of the propellant [26-27]. A study conducted by Kumar et al. [27] artificially introduced cracks into a composite propellant to better understand the mechanisms that cause defective propellants to explode. The researchers observed that in certain cases, high-pressure and high-temperature gases can penetrate into a crack in the propellant. If enough energy from the high-pressure and high-temperature gases is transferred into the crack, the interior of the propellant will begin to burn. As the interior of the propellant is burning, it will generate and buildup additional high-pressure and high-temperature gases which can cause the propellant to explode. The researchers also determined that even if the propellant does not explode under these conditions, the performance of the propellant will be significantly altered.

Because so many different factors during the manufacturing process can cause voids and reduce density in propellants, understanding their impact on rocket performance and safety is an

important topic of research. Foltran et al. [15] conducted a study on how propellants manufactured in a mechanical press impacted the density and burning rate of potassium nitrate (KNO_3)/sucrose ($C_{12}H_{22}O_{11}$) propellants. After the propellant ingredients were ground and mixed, they were loaded into a punch and die before being placed in a hydraulic press. The hydraulic press' compression pressures were varied between 16, 24, 32, 48, 64, 72, and 80 MPa to determine how compression pressure affected the densities and burning rates of potassium nitrate/sucrose propellants. Once the propellants were removed from the punch and die, their densities were determined by weighing the samples and calculating the volume by measuring the geometric dimensions of the propellants. As the researchers expected, an increase in the hydraulic press' compression pressure resulted in an increase in propellant density. For a potassium nitrate/sucrose propellant free of any voids, the TMD is 1.888 g/cm^3. Using the second-order polynomial function developed by the researchers to model propellant density as a function of compression pressure, they were able to achieve a maximum sample density of 1.650 g/cm^3, or 87.39% of TMD at the maximum compression pressure of 80 MPa. While at the minimum compression pressure of 16 MPa, the sample density was calculated to be 1.412 g/cm^3, or 74.79% of TMD. The propellants were also tested for burning rate where an increase in compression pressure, and thus increase in propellant density, resulted in a decrease in burning rate. Another second-order polynomial function was developed by the authors to model burning rate as a function of compression pressure. The maximum burning rate was calculated to be 0.106 in/s at a minimum compression pressure of 16 MPa, while the minimum burning rate was calculated to be 0.091 in/s at a maximum compression pressure of 80 MPa. This effect of increasing compression equates to approximately a 15% difference in burning rate from the lowest- to highest-density propellant. These results agree with similar works done on potassium

nitrate/sucrose propellants conducted by Aravind et al [28], Nakka et al. [29], and Vyverman et al. [30]. These results are an indication that voids and low densities in propellants can result in an increase in propellant burning rate.

In a separate study conducted by McClain et al. [16], propellant performance and quality were compared between two different manufacturing methods. The researchers compared propellants manufactured through a traditional casting method to propellants that are manufactured using additive manufacturing techniques. Two different AP-based propellants with 85% solids loading were used in the experiment. The first propellant formulation used the traditional R45M HTPB as the binder material, while the other formulation used the Illumabond 60-7105 UV-curable polyurethane binder. Both propellant formulations were manufactured using both the casting and additive manufacturing methods to better understand how the different manufacturing methods and binder materials would affect the quality of the propellants. The measured densities of the cast and printed HTPB propellants were 86.3% and 92.3% of the TMD, respectively. The measured densities of the casted and printed UV-cured propellants were 89.6% and 101.2% of the TMD, respectively. In both propellant formulations, the printed propellants displayed higher densities than the cast propellants. In addition, through the use of x-ray radiography, the researchers were able to determine that the UV-cured propellants had significantly fewer voids than the HTPB propellants. This result supports the theory that void formation can be caused by chemical reactions between the HTPB binder and other propellant chemicals as the UV-curable binder does not form any volatiles as it cures. The propellants were tested for burning rate where the cast propellants with lower densities had higher burning rates than the printed propellants with higher densities. The researchers determined that the increase in burning rate is due to the significantly higher number of voids found in the cast propellants.

In summary, voids developed in propellants during the manufacturing process are the main culprits in reducing propellant densities below their TMD. Previous work conducted by various researchers have shown that within identical propellant formulations, propellants with lower densities will routinely have higher burning rates compared to propellants with higher densities. This relationship between propellant density and burning rate is relatively established in the literature. However, burning rate data are usually only taken a few times throughout a pressure range to form a burning rate curve. Little research has been conducted to statistically analyze how burning rate variance and magnitude are affected by propellant density. Further studies are needed to better understand the relationship between voids, propellant density, and burning rate. Additionally, the effect of manufacturing variances and procedures utilized within the Petersen Research Group at Texas A&M University, particularly with regard to TMD and corresponding burning rate, had until the present thesis not been formally quantified. Hence, a thorough assessment of the procedures in the author's laboratory were desired.

CHAPTER III

PROPELLANT FORMULATIONS

Propellant Formulation Test Matrix

The composite solid propellants studied in this thesis were a baseline propellant formulation containing ammonium perchlorate (AP) as the oxidizer, R45M hydroxyl-terminated polybutadiene (HTPB) as the fuel/binder, and isophorone diisocyanate (IPDI) as the curative. The propellants used in this study consisted of both monomodal and bimodal AP particle size distributions. A monomodal propellant consists of a single, distinct AP particle size, while a bimodal propellant uses two distinct AP particle sizes. The bimodal propellants were tested at various pressures between 500 and 2500 psia to develop full burning rate curves. The monomodal propellants were tested for burning rate at a low (~500 psia) and high (~3000 psia) pressure point to examine how propellant density affects the variance of burning rate at both low and high pressures.

Table 2 lists the different propellant formulations that were tested in this thesis. The bimodal propellants were separated into different density groups based on the different extrusion methods that have been refined to consistently produce low-, medium-, or high-density propellants. The monomodal propellants were separated into different density groups based on their densities relative to the TMD. Propellants with densities greater than or equal to 95% TMD were considered high-density propellants, whereas propellants with densities lower than 95% TMD were considered low-density propellants. Note that the terms low-, medium-, and high-density propellants can be subjective based on the application as well as the manufacturability of the propellant.

Table 2: Propellant formulations used in this thesis.

AP Distribution	Solids Loading (%)	AP Particle Size (µm)	Propellant Density		
			TMD (g/cm^3)	Actual (g/cm^3)	Group (% TMD)
Bimodal	75%	200/20 (70%:30%)	1.517	~1.477	High (~97% TMD)
Bimodal	75%	200/20 (70%:30%)	1.517	~1.447	Medium (~95% TMD)
Bimodal	75%	200/20 (70%:30%)	1.517	~1.398	Low (~92% TMD)
Monomodal	77%	200	1.545	≥1.468	High (≥95% TMD)
Monomodal	77%	200	1.545	<1.468	Low (<95% TMD)

In Table 2, the AP particle sizes are listed based on the information provided by the suppliers or estimated by the researchers. A container of AP purchased off the shelf will generally have a normally distributed range of AP particle sizes instead of one, single particle size. Because of this, the suppliers usually label different containers of AP based on their approximate, average AP particle size. However, batch-to-batch variations during the AP milling and sieving process can lead to small disparities between the stated and actual average AP particle sizes. The 200-µm AP used in this thesis was manufactured by American Pacific Fine Chemicals (AMPAC) and was taken directly from the container without going through any additional sieving processes. The 20-µm AP was manufactured through a sieving process developed by the Petersen Research Group. The sieving procedure began by placing a small quantity of 90 µm AP manufactured by AMPAC into a stack of 90-, 75-, and 25-µm sieves. This sieve stack is then placed into a Resodyn acoustic mixer, shown in Fig. 7, to sieve the AP into different particle size ranges. The AP particles are sieved for two minutes at 15 g's of

acceleration to ensure the AP particles are thoroughly dispersed. This process is repeated until enough AP material has been collected to manufacture the propellants.

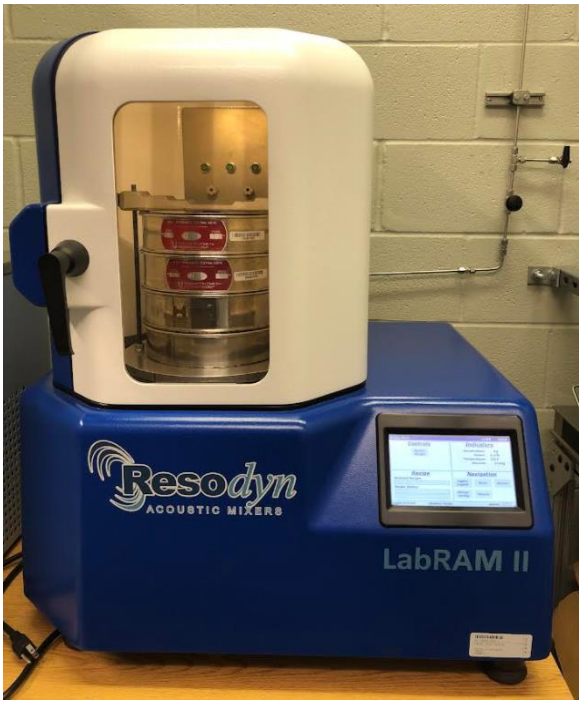

Figure 7. Resodyn acoustic mixer loaded with sieve stack to sieve AP particles into desired particle size ranges.

As previously mentioned, the containers of both sieved and unsieved AP will contain a normally distributed range of AP particle sizes. Therefore, it is important to determine the average particle size and distribution of the AP since propellant burning rate is highly correlated to AP particle size. A propellant with smaller AP particles will have a higher burning rate than a similar propellant with larger AP particles. Smaller AP particles will cause a propellant to burn faster as its higher surface area-to-volume ratio stimulates the formation of premixed flames while larger AP particles will promote a diffusion flame [31]. A premixed flame will burn hotter and faster than a diffusion flame, which is why propellants with smaller AP particles will have a higher burning rate [32]. However, smaller AP particles will tend to agglomerate into larger particles if not properly stored. A study of the particle distribution will help indicate if these

agglomerates are present in the propellant samples which can negatively affect their burning rates. A Beckman-Coulter particle sizing apparatus, shown in Fig. 8, was used to determine the distribution of AP particle sizes used in the propellants.

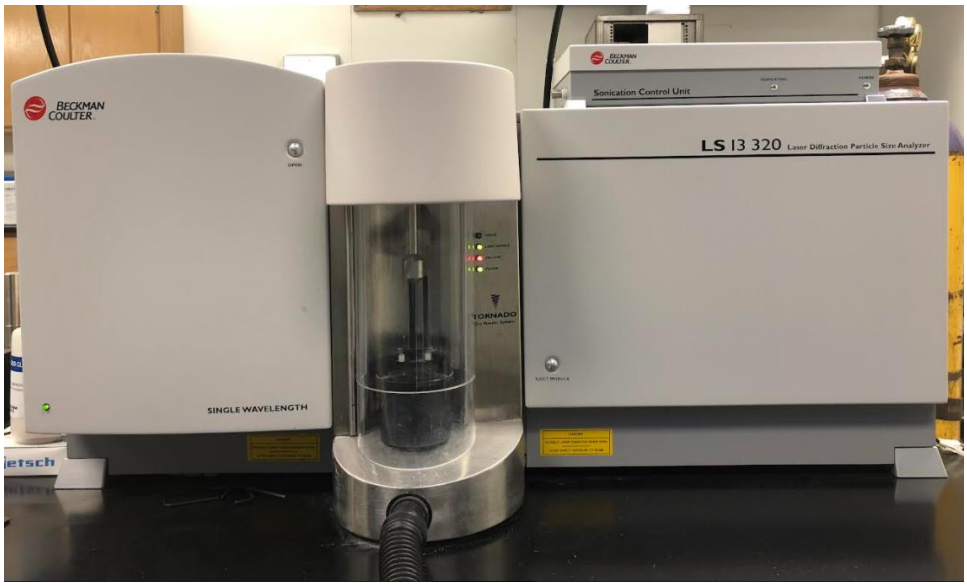

Figure 8. Image of Beckman-Coulter apparatus used to particle size the AP.

The particle size distribution of the 200- and 20-µm AP are shown in Fig. 9 and Fig. 10, respectively. Although the nominal sizes of AP used are 200 and 20 µm, the measured, average AP particle sizes are approximately 224 µm and 25 µm, respectively. The results indicate that the AP that was used for this thesis was relatively normally distributed and similar to their nominal sizes. Since the particle sizes are slightly higher than expected, the burning rate is expected to slightly decrease. However, since every propellant used in this thesis was manufactured from the same source of AP, the burning rate results relative to each propellant formulation were not affected.

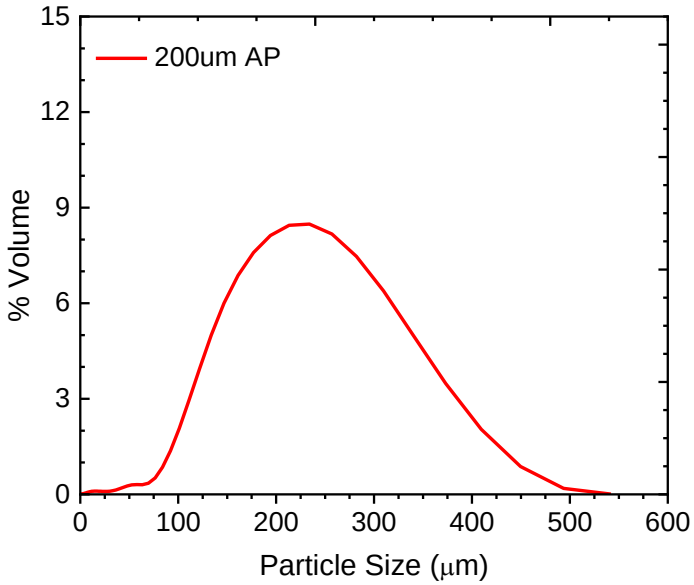

Figure 9. Particle size distribution plot of 200-µm AP.

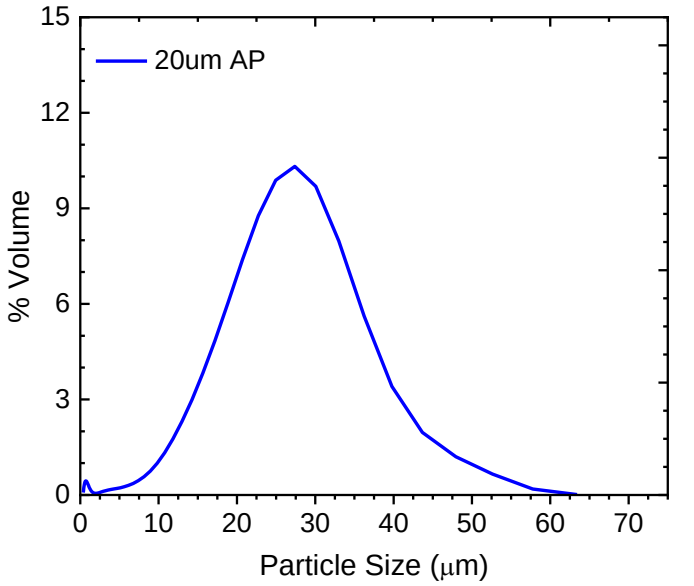

Figure 10. Particle size distribution plot of 20-µm AP.

Propellant Mixing

As previously mentioned, composite solid propellants manufactured in the industry are normally mixed in vacuum-sealed planetary mixer to form a viscous propellant slurry. However, a hand mixing procedure is used in this thesis since the Petersen Research Group manufactures composite solid propellants on a small, laboratory-scale basis. The use of large-scale industrial mixers would lead to wasted material as the propellants used in this thesis are a fraction of the size of those used in the industry. Figure 11 depicts a propellant slurry that has been hand mixed in a laboratory beaker. Propellant ingredients are mixed in one at a time with intermediate vacuuming between each solid ingredient. This hand-mixing procedure has been refined through years of testing and produces comparable propellants to those mixed in an industrial mixer [24].

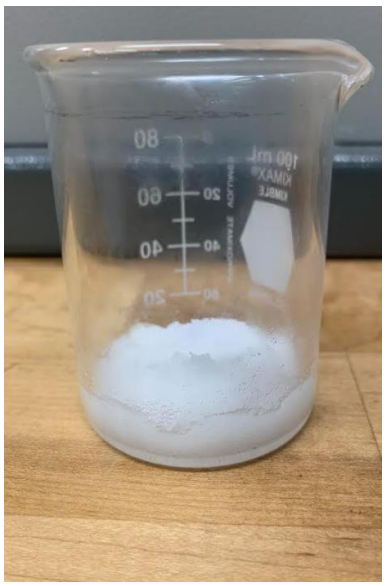

Figure 11. Image of hand-mixed AP/HTPB propellant slurry.

The propellant mixing process begins by using acetone to sterilize a glass beaker and glass stirring rod. The glass beaker is then placed on a scale where liquid ingredients, such as HTPB, are weighed on a scale with a resolution of 0.01 g. If the formulation calls for any additional liquid ingredients, they are usually added to the beaker prior to the solid ingredients.

The exception to this is IPDI, which must be the last ingredient to be added, otherwise the curing process will initiate prematurely. Adding all the liquid ingredients prior to the solid ingredients, except for IPDI, ensures a uniformly mixed propellant matrix material that will be evenly distributed throughout the propellant. When each liquid ingredient is added to the beaker, it is mixed for 10 minutes to ensure the mixture is uniform. The addition of solid ingredients occurs once all the liquid ingredients, except IPDI, have been completely and uniformly mixed. The order that solid ingredients are introduced into the mixture is dependent on their particle size. The smallest particles are mixed first. They are then followed by increasingly larger particles which allow for the smaller particles to be more evenly distributed throughout the mixture and fill in the voids between larger particles. Each solid ingredient is mixed for 10 minutes before being placed in a vacuum chamber for 20 minutes. Placing the mixture into a vacuum helps remove pockets of air trapped in the propellant slurry as well as any possible volatiles created from interactions between different chemicals. All mixing is conducted on a hot plate set at approximately 65℃. Heating the mixture reduces its viscosity, resulting in an easier and more thorough mixing process.

The monomodal propellants used in this thesis were manufactured using the 200-μm AP (measured AP particle size of 224 μm) at a 77% oxidizer content. The bimodal propellants had a 75% oxidizer content and were manufactured by mixing the 200- and 20-μm AP (measured AP particle sizes of 224 and 25 μm, respectively) at a 70/30 coarse-to-fine AP ratio by mass. These propellants contained a lower oxidizer content by mass compared to the industry standard of 85% oxidizer content because propellants with lower solids loading are easier to manufacture and can achieve densities closer to the TMD.

Propellant Extrusion

Once every propellant ingredient has been thoroughly mixed together and allowed to vacuum, the next step in the manufacturing process is to extrude the propellant. The Petersen Research Group normally hand extrudes propellants into Teflon® tubing with a 0.1875-in inner diameter. The Teflon® tubing packed with propellant is then cut into strands approximately 1-inch in length before being placed into a laboratory oven where they will cure for 7 days at 63°C. Figure 12 shows several hand-extruded propellant samples that have been cut to 1-inch in length prior to curing.

Figure 12. Hand-extruded propellant samples cut to approximately 1-inch in length.

Although hand-extruded propellants have been found to produce comparable propellants to those that are cast or extruded with different methods, a custom propellant extruder was designed by the author and tested to mechanically extrude propellants. This custom extruder allows for the Petersen Research Group to produce high-quality propellants that can achieve higher densities and contain fewer voids than those that are extruded by hand. Additionally, this custom extruder can be adjusted to allow for low-quality propellants with low densities and numerous voids to be produced. This customization allows for a higher level of control during the manufacturing process which created a more efficient way of producing propellants with

varying densities for the present thesis. This custom extruder also created an opportunity for the Petersen Research Group to compare the performance of hand-extruded propellants to those that are mechanically extruded to determine if there is a significant difference between the two extrusion methods.

A custom syringe, shown in Fig. 13, was designed to hold and extrude propellant slurry into Teflon® tubing with an inner diameter of 0.1875 in. This custom syringe was designed using 304 stainless steel due to its inert nature, corrosion resistance, and good mechanical properties. The syringe tip is designed with a gentle taper to minimize flow resistance when the propellant slurry is being extruded. A barbed hose connection was manufactured onto the syringe tip to allow for the Teflon® tubing to be securely attached to the custom syringe. The syringe tip is fully removeable which makes loading the propellant slurry easier and simplifies the cleaning process once extrusion is complete. The flange on the syringe tip allows for a 1.5-in compression nut to securely attach the syringe tip to the body of the syringe. A rubber gasket can be added between the syringe tip and body to ensure an airtight seal. The syringe plunger was precision machined and fitted with a size 206 Viton® O-ring to prevent propellant slurry from leaking past the plunger. A custom insert can be loaded into the syringe before the plunger which allows for a larger quantity of propellant slurry to be extruded into the Teflon® tubing. Without this custom insert, a large quantity of propellant slurry would be trapped in the syringe tip with no way to extrude it. Further details on the extruder design shown in Fig. 13 can be found in the Appendix.

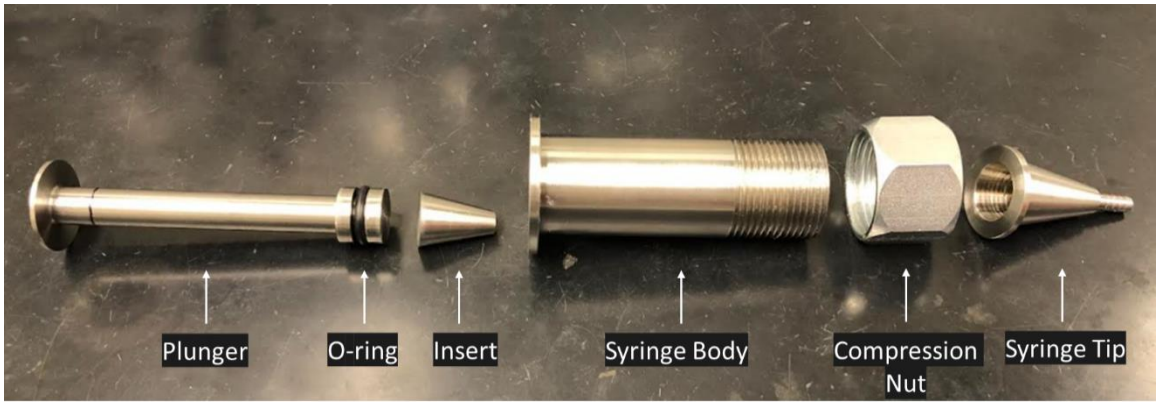

Figure 13. Image of the custom syringe components designed to extrude propellant slurry into a Teflon® tubing casing.

To mechanically extrude propellants, the propellant slurry is first loaded into the body of the syringe. Once the propellant slurry has been loaded, the syringe tip is aligned and placed atop the syringe body. The compression nut is then placed over the flange of the syringe tip and screwed onto the body of the syringe to secure it into place. The custom insert is placed into the syringe body and followed by the plunger and O-ring assembly. Next, the Teflon® tubing is securely attached to the barbed hose connection on the syringe tip. The assembled custom syringe is then loaded into a New Era NE-8000 high-pressure syringe pump which will apply the force needed to extrude the propellant slurry. A vacuum pump can be attached to the end of the Teflon® tubing to remove air from the system to produce high-density propellants. However, if the goal is to produce low-density propellants, the vacuum pump can be removed to intentionally introduce air into the system to promote the formation of voids in the propellant. Figure 14 depicts a schematic of the mechanical extrusion method used for this thesis.

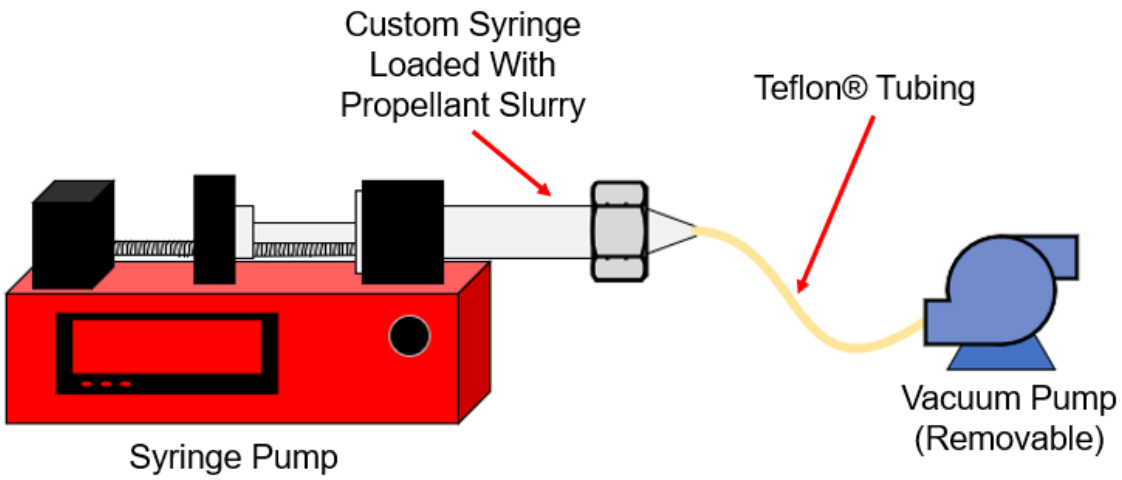

Figure 14. Schematic of the mechanical extrusion process. The vacuum pump is used to remove air from the system to create high-density propellants. Removing the vacuum pump creates low-density propellants by promoting the formation of voids.

The baseline propellants manufactured for this thesis were moderately translucent, which allowed voids in the propellants to be visible. Figure 15 depicts the low-, medium-, and high-density 75% bimodal propellants with different amounts of visible voids. As expected, the propellants with lower densities had more-visible voids than the propellants with higher densities. This void visibility is because the contents of the voids have a much lower density than the ingredients used in a propellant. These images were captured during burning rate testing with a high-speed camera, further discussed in the next chapter.

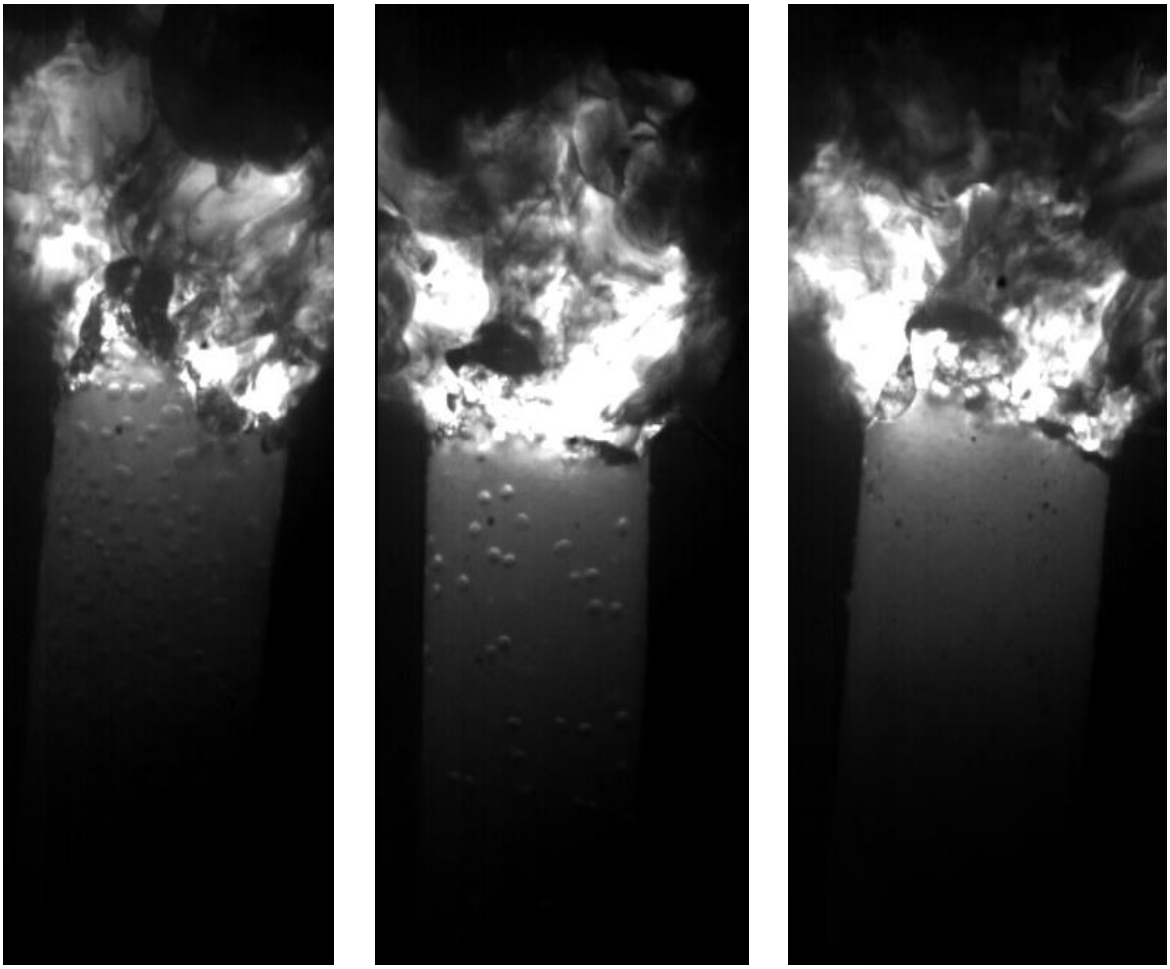

Figure 15. Left: Low-density propellant with numerous voids. Middle: Medium-density propellant with moderate quantities of voids. Right: High-density propellant with no visible voids.

CHAPTER IV

TESTING PROCEDURES

Sample Preparation

Once the propellants are fully cured, they are removed from the oven and carefully cut from their Teflon® casing. The propellant sample's mass and length are then measured to determine their densities. A digital caliper with a resolution of 0.0005 in is used to measure the dimensions of the propellant sample to calculate its volume. Even though the inside diameter of the Teflon® tubing is 0.1875 in, the calipers are still used to verify the diameter of the propellant at several locations. The densities of the propellants are then determined by using the mass and calculated volume of the cylindrical propellants. This caliper method of determining propellant density is often used in the literature and has been shown to be relatively precise and reliable. However, human errors when using calipers to determine the dimensions of the propellant can considerably affect the calculated density. In addition, if the top and bottom ends of the propellant sample are not cut perfectly straight, there will be a small gap in the sample that will provide an inaccurate calculation of the propellant volume. This small gap will artificially increase the sample's volume and therefore, artificially decrease its density. Furthermore, since the propellants used in this thesis are relativity elastic, pressing too hard on the calipers can cause the propellant samples to bend slightly. This bending will artificially decrease the volume and therefore, artificially increase the propellant density. Figure 16 depicts several of many possible outcomes when performing caliper measurements on a propellant sample.

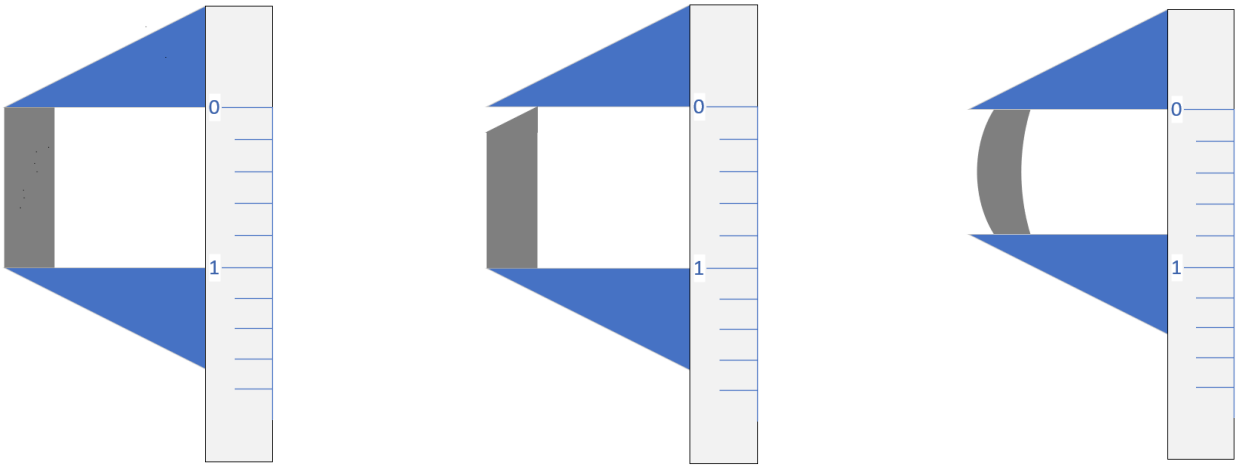

Figure 16. Left: Ideally cut propellant with proper length measurement. Middle: Gap at the top of the propellant will artificially decrease the propellant density. Right: Excessive compression of the calipers will bend the propellant and artificially increase the propellant density.

For this thesis, another method with less potential for human error was developed to determine the density of the propellant. This method is based on the Archimedes' principle that states when a body is fully submerged in a fluid, it will displace a volume of the fluid equal to the volume of the body. If the density of the fluid is known, the mass of the displaced fluid can be used to calculate the volume of the displaced fluid and, thus, the volume of the body. The Archimedes' method was used to determine the volume of the propellant by suspending the propellant in a beaker of HTPB. Traditionally, water is used as the fluid medium, but HTPB was used instead because the AP oxidizer in the propellant is soluble in water. The beaker of HTPB was placed on a scale where the mass of the displaced HTPB could be measured to determine the volume of the propellant. It is crucial that the propellant is suspended in the HTPB rather than sitting on the bottom of the beaker. If the propellant is suspended in HTPB, only the mass of the displaced HTPB is measured. But if the propellant is on the bottom of the beaker, the mass of the propellant is also taken into account. The propellant mass and volume are then used to calculate the density of the propellant. Since this method relies on the use of a scale to determine the

propellant volume, the likelihood of human error is significantly reduced. Figure 17 depicts an image of the apparatus in addition to a detailed schematic of the tools used to determine the propellant sample volume using Archimedes' principle.

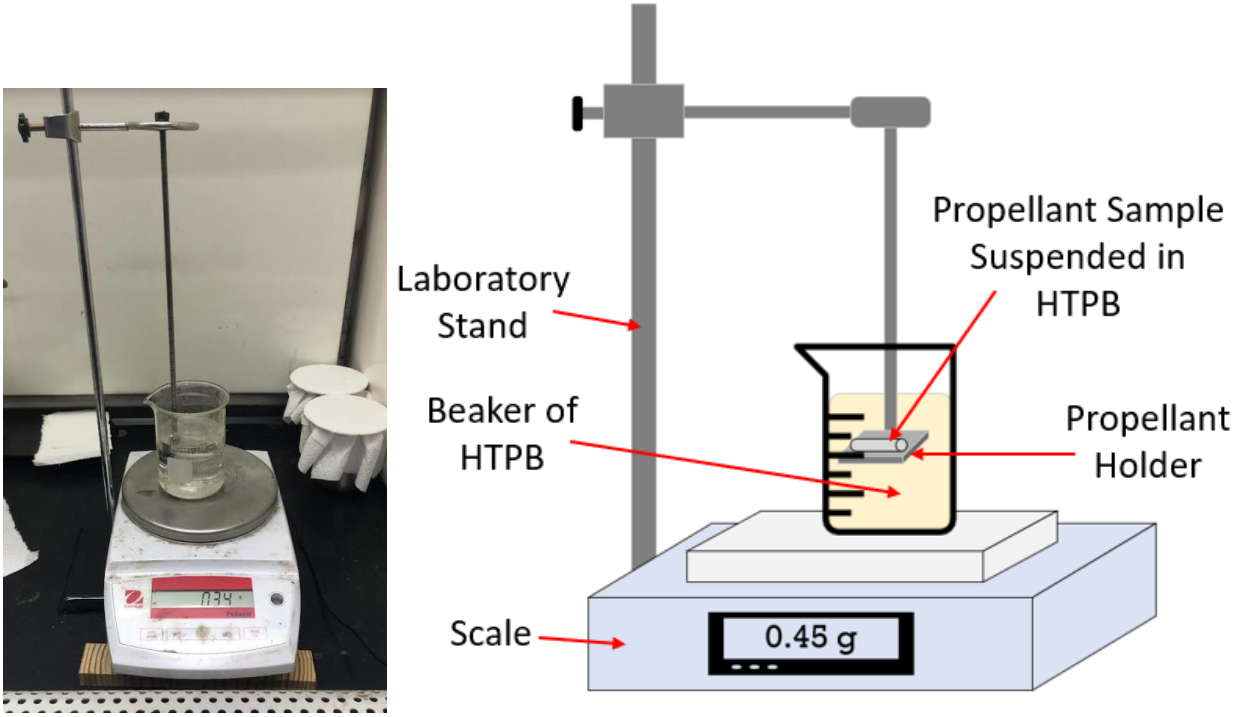

Figure 17. Left: Image of apparatus used to determine propellant sample density using Archimedes' principle. Right: Detailed schematic of the apparatus design.

Prior to testing, the sidewall of the cured propellant sample is coated with a thin layer of HTPB that acts as a burn inhibiter. Coating the sidewall of the propellant with HTPB reduces the likelihood of the propellant burning on the side and ensures a linear burn in the axial direction of the propellant. Figure 18 depicts a propellant that is burning on its sidewall which can provide an inaccurate measurement of the propellant burning rate.

Figure 18. Image of propellant burning on its sidewall.

Once the propellant is coated in HTPB, a small Teflon® tube collar is attached to the bottom of the propellant to add stability and prevent the propellant from tipping over in the sample holder. The propellant is then loaded into a bolt-shaped sample holder with two hook-shaped metal leads. A nichrome wire is set across the two metal leads and pressed into (slightly) the surface of the propellant. This nichrome wire is part of the propellant ignition system used to initiate the combustion process. A size 75 Viton® O-ring is placed into a groove on the bolt-shaped sample holder to create an airtight seal when it is loaded into the test vessel. Thread Teflon® tape is also wrapped across the threads of the sample holder to provide additional sealing. Figure 19 depicts an image of a prepared sample holder as well as a detailed schematic of its components.

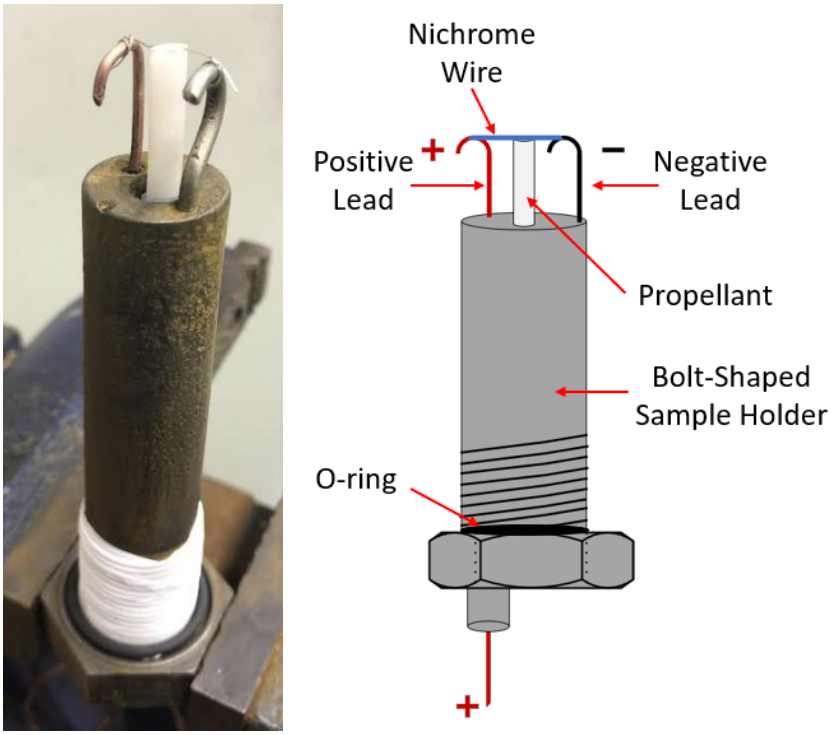

Figure 19. Left: Photograph of prepared propellant sample loaded into the sample holder. Right: Schematic of the sample holder and its main components.

Test Vessel

Once the propellant and sample holder have been fully prepared, the sample holder is bolted into the test vessel. The test vessel, also known as a strand burner, is a constant-volume high-pressure vessel that can test propellants at pressures up to 6000 psia. The Petersen Research Group also has a second pressure vessel developed by Dillier et al. [33] that is rated for tests up to 10,000 psia. However, this very-high pressure strand burner was not used for this thesis. The high-pressure strand burner that was used in this thesis to test propellants for burning rate is shown in Fig. 20. This strand burner is pressurized with ultra-high purity nitrogen gas from a K-size gas cylinder to alter the chamber pressure at which the propellant burns. Ultra-high purity nitrogen is used to pressurize the system as it is inert and will not affect the combustion process

of the propellant. The plumbing system on the strand burner is fitted with both manual and pneumatic valves to control the flow of nitrogen in and out of the strand burner.

The strand burner is fitted with three windows on the side which allow for high-speed video, spectroscopic, and light-trace data to be recorded. A fourth window located on the top of the strand burner allows for laser ignition of the propellant when ignition timing data are of importance. Pressure transducers are also installed in the testing apparatus to evaluate the chamber pressure and how it behaves as the propellant is burning. Due to the inherent dangers of testing under high pressures, the strand burner is located in a blast-proof room. A ventilation system is also located in the testing facility to remove any hazardous gases that are generated as a by-product of combustion. In the event of a power outage, the pneumatic valves have been set to be normally closed to prevent overpressurization or a rapid depressurization in the system. Manual safety vent valves can then be used to safely depressurize the system. In addition, the design of the plumbing and control systems allows for the pressurization, depressurization, and ignition processes to be initiated in the safety of a separate control room.

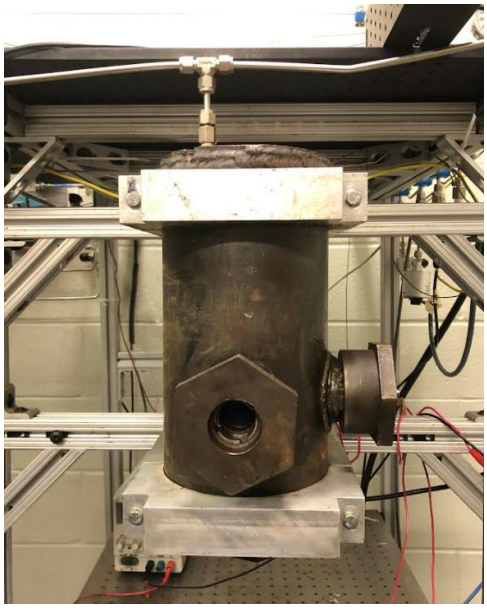

Figure 20. Photograph of the high-pressure strand burner used to experimentally determine the burning rates of propellants.

Testing and Data Acquisition

Ignition of the solid propellant is initiated by energizing the nichrome wire that sits across the propellant and two metal leads of the sample holder. There is a switch in the circuit that allows the researchers to control when the ignition process can be initiated. When the switch is activated, the circuit is complete, and a voltage is sent across the wire where it will reach temperatures near 1000℃ to initiate the combustion of the propellant. When ignition of the propellant is initiated, data are recorded by the data acquisition (DAQ) system with the computer located in the control room. A schematic of the test vessel, DAQ system, and primary plumbing routes are shown in Fig. 21.

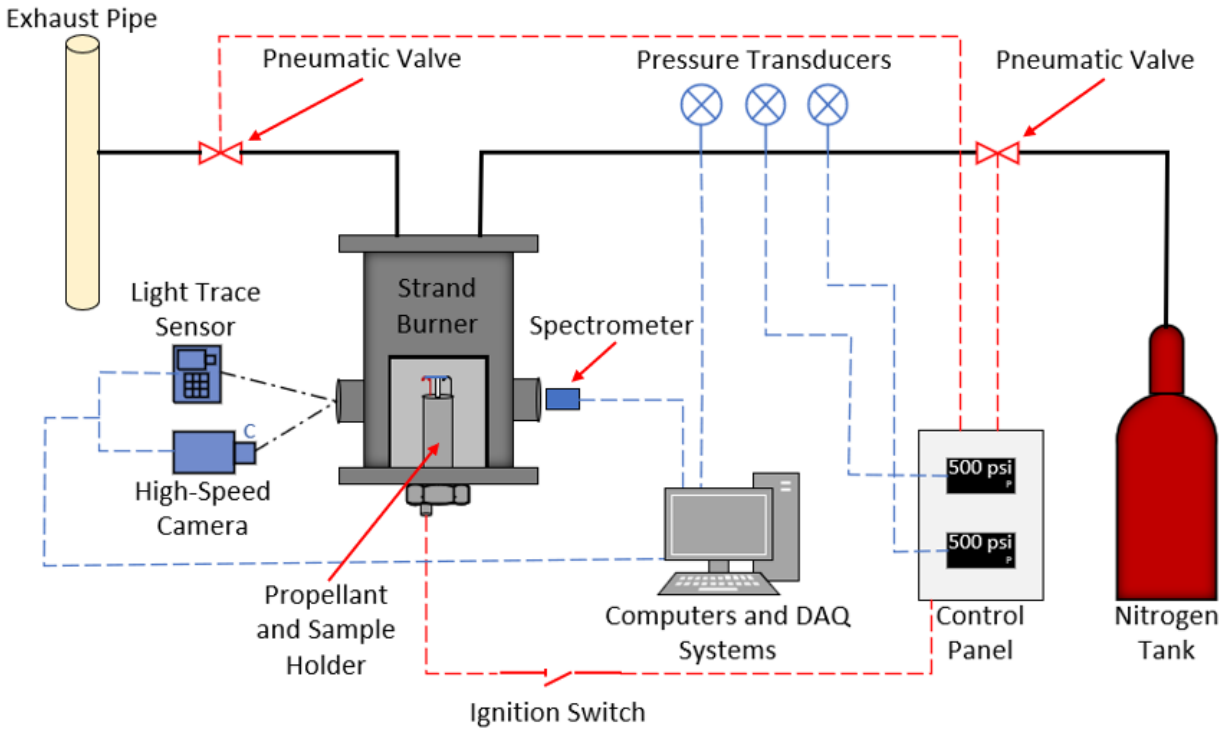

Figure 21. Schematic of testing apparatus used to determine propellant burning rates.

A high-speed camera is used to capture footage of the propellant burning at 500 fps. A higher frame rate can be selected if needed. The spectroscopic data are processed through the DAQ system to provide information and measurements of the different products of combustion. In total, there are three pressure transducers that have been installed onto the system to ensure accurate pressure measurements. The first pressure transducer is connected to the DAQ system and captures the change in pressure as the propellant is burning. The second pressure transducer is connected to a digital pressure transducer display in the control room that provides synchronal pressure readings of the combustion chamber to get an approximation of the testing pressure prior to ignition. This pressure transducer can also be used to determine if propellant combustion has been achieved as there will be a noticeable rise in pressure as a result of the burn. The third pressure transducer is connected to another digital pressure transducer display and is also used to calibrate the two pressure transducers that were previously mentioned. This calibration pressure transducer is needed because the other two pressure transducers are exposed to products of combustion that can degrade them over time. The calibration pressure transducer is only exposed to the inert nitrogen gas and is closed off from the system before propellant ignition occurs. The data provided from the first pressure transducer as well as the light trace sensor are processed through a DAQ system to determine propellant burn time. The measured propellant length and burn time are then used to calculate the propellant burning rate. Figure 22 depicts an example of the pressure and light-trace data and how they are used to determine propellant burn time.

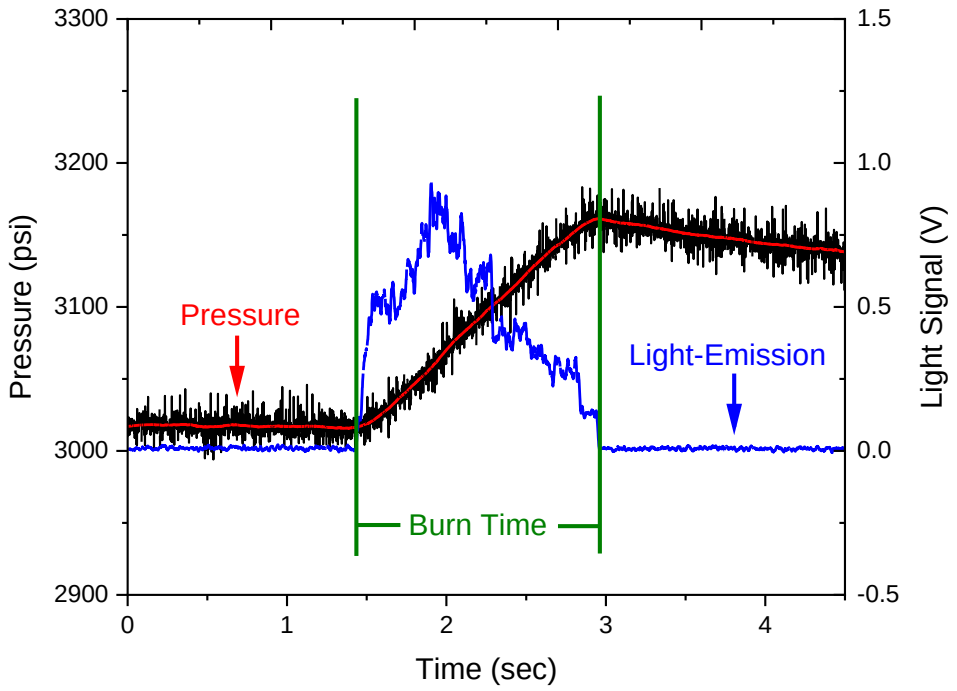

Figure 22. Example of pressure and light-emission intensity data that are used to determine propellant burn time.

Omega PX359-7.5KG5V pressure transducers are used to detect the pressure of the system while a New Focus 2031 photoreceptor is used to detect the light-emission intensity levels. The pressure and light-emission intensity data are collected using a DAQ board from Gage Applied Sciences and their accompanying GageScope software. The data are captured at a sampling rate of 1 kHz over a 10 second period to ensure the whole burning process is recorded. When propellant combustion is initiated, there will be a sharp increase in both the pressure and light-emission intensity. During the duration of combustion, the pressure will steadily increase, but the light-emission intensity can vary depending on the location and structure of the flame. But once combustion has concluded, the pressure will begin to decrease, and the light-emission levels will return to a steady-state. These changes in pressure and light-emission intensity are

used to determine the total time needed for the propellant to completely burn. However, if the smoothed pressure trace is not perfectly linear, a line that best represents the linear burning behavior of the propellant will be drawn by the researchers to determine the ideal burning time of the propellant. The pressure transducer data can sometimes be difficult to interpret due to the background noise as shown from the black lines in Fig. 22. A Savitsky-Golay smoothing filter, shown as the red line in Fig. 22, is applied to the original pressure data to filter out some of the higher-frequency noise and provide a more legible pressure trace.

CHAPTER V

PROPELLANT EXPERIMENTAL DATA

Burning Rate and Density Data

Baseline AP/HTPB propellants were measured for their densities and experimentally tested for their burning rates. Propellant densities were measured using the Archimedes' method as there are fewer opportunities for human error. The bimodal propellants were tested at several pressures between 500 and 2500 psia to determine how the burning rate curve would be affected by different propellant densities. Monomodal propellants were experimentally tested for burning rates at approximately 500 and 3000 psia to gather statistical data on how variations in propellant density will affect the magnitude and variance of burning rates in both low- and high-pressure regions. Propellants were manufactured using both the traditional hand extrusion and newly developed mechanical extrusion methods to determine if there are any differences in densities and burning rates between the two extrusion methods.

Both the caliper and Archimedes' methods of density measurements were tested for precision using elemental cubes of copper with a purity of 99.95%, nickel with a purity of 99.6%, and lead with a purity of 99.99% as shown in Fig. 23.

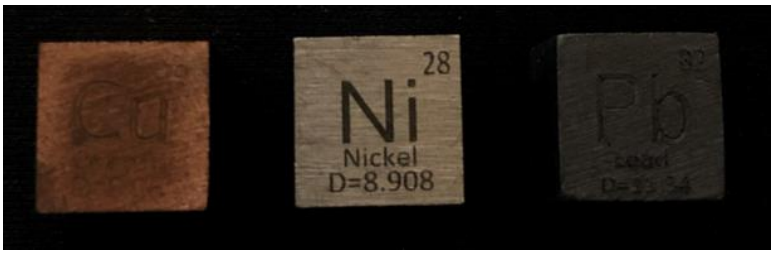

Figure 23. Elemental cubes of copper, nickel, and lead used to compare the precision of the caliper method and Archimedes' method of determining densities.

Using the caliper method, the volume was calculated by taking measurements of the length, width, and height of each elemental cube. With the Archimedes' method, the elemental

cubes were suspended in a beaker of HTPB where the mass of the displaced HTPB was used to calculate the volume of each elemental cube. The mass of each elemental cube was measured using a laboratory scale for both the caliper method and Archimedes' method. Table 3 shows how both methods performed when determining the density of each elemental cube. Calculating the densities of the copper, nickel, and lead elemental cubes using the caliper method resulted in a precision of 97.58%, 98.01%, and 97.91%, respectively. While using the Archimedes' method to calculate the densities of the copper, nickel, and lead elemental cubes yielded a precision of 97.99%, 98.10%, and 98.30%, respectively. This experiment shows that both methods of determining density yield similar and precise results, although the Archimedes' method is slightly more precise. However, these elemental cubes were rigid, and the edges sat almost perfectly flush with the calipers. Using calipers to measure the dimensions of propellant samples can yield various problems as propellants can be flexible, and the edges may not sit perfectly flush against the calipers. Because of the results of this experiment and the potential human errors associated with measuring the dimensions of propellants using calipers, the Archimedes' method was selected as the method of choice when determining the density of each propellant sample.

Table 3: Table comparing the caliper and Archimedes' methods of determining the densities of copper, nickel, and lead elemental cubes.

Element	Mass (g)	Actual Density (g/cm^3)	Caliper Density (g/cm^3)	Archimedes Density (g/cm^3)	Caliper Method Precision (%)	Archimedes' Method Precision (%)
Copper (99.95%)	8.77	8.960	8.743	8.780	97.58%	97.99%
Nickel (99.6%)	9.02	8.908	8.731	8.739	98.01%	98.10%
Lead (99.99%)	11.63	11.340	11.104	11.147	97.91%	98.30%

The bimodal propellants were manufactured using both the hand extrusion and mechanical extrusion processes. Table 4 shows the different extrusion methods and the results from their density measurements. A total of 14 propellant samples were manufactured for each density group. The hand extrusion process was used to create medium density propellants by hand-pressing the propellant slurry into Teflon® tubing with a 0.1875-in inner diameter. This method produced medium-density propellants with an average density that was 95.40% of the TMD. To create low-density propellants, the custom syringe and syringe pump were used without the vacuum pump to deliberately introduce air into the system. This method created low-density propellants that had an average density that was 92.13% of the TMD. High-density propellants were created using the same custom syringe and syringe pump, but with the vacuum pump attached to remove air from the system. This method created high-density propellants with an average density that was 97.34% of the TMD.

Table 4: Table comparing the densities of different extrusion methods for the 75% bimodal propellants burned between 500 and 2500 psia.

75% Bimodal Density Group	Extrusion Method	TMD (g/cm^3)	Average Density (g/cm^3)	Average Density (% TMD)
Low Density	Pump Extrusion w/ Air	1.517	1.398	92.13%
Medium Density	Hand Extrusion	1.517	1.447	95.40%
High Density	Pump Extrusion w/ Vacuum	1.517	1.477	97.34%

Figures 24, 25, and 26 display the burning rate curves for the low-, medium-, and high-density 75% bimodal propellants, respectively. Two separate batches of low-, medium-, and high-density bimodal propellants were burned at similar pressures to determine if the results

were repeatable. Samples that displayed burning rates that were deemed as outliers were removed from the plot so the burning rate curve would not be improperly manipulated. Because of this, the low-density propellants had one outlier point that was removed from the plot. Since the burning rate curves between each batch are comparable, these results indicate that all three propellant density groups can produce repeatable burning rate results despite their manufacturing method and overall average density, within the ranges of TMD in this study.

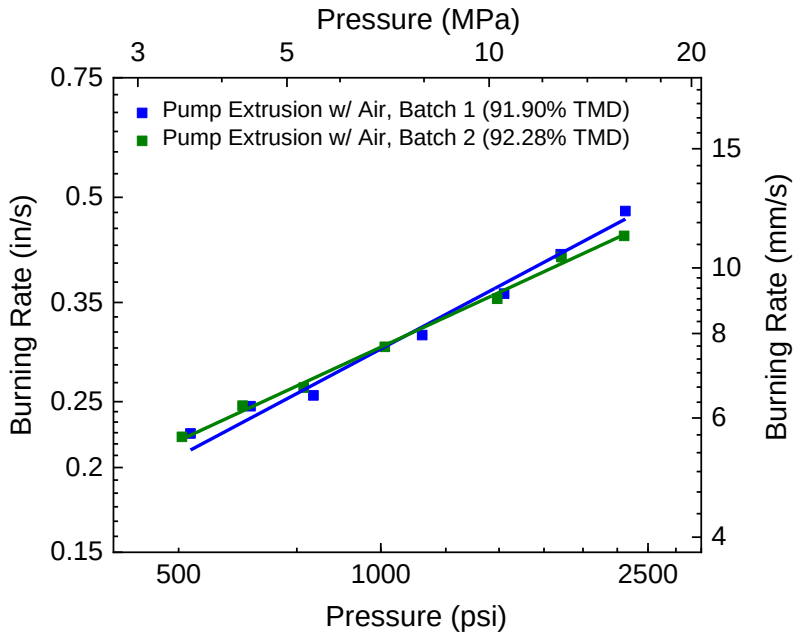

Figure 24. Burning rate plot of the 75% bimodal propellant manufactured using mechanical extrusion while exposed to air to create low-density propellants. The two groups had an average density that was 92.13% of the TMD.

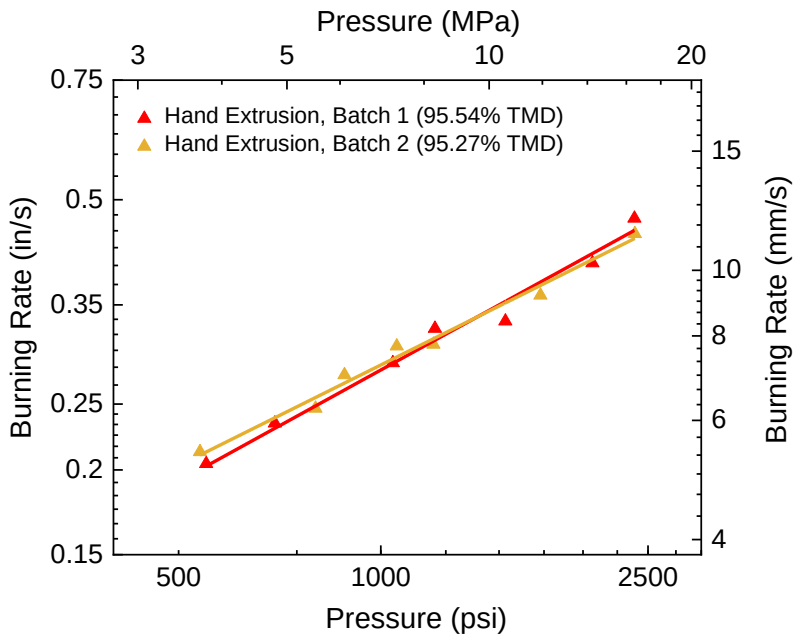

Figure 25. Burning rate plot of the 75% bimodal propellant manufactured using hand extrusion to create medium-density propellants. The two groups had an average density that was 95.40% of the TMD.

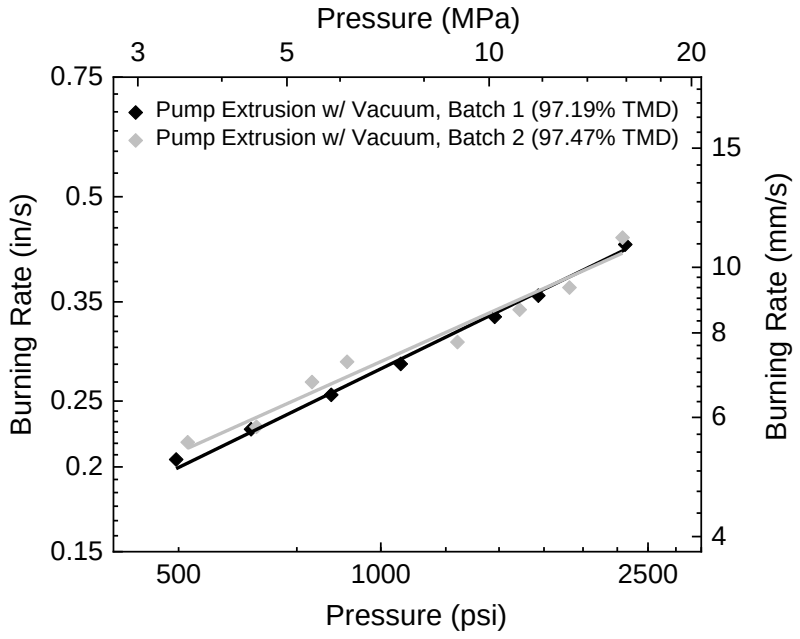

Figure 26. Burning rate plot of the 75% bimodal propellant manufactured using mechanical extrusion while under vacuum to create high-density propellants. The two groups had an average density that was 97.34% of the TMD.

Figure 27 compares the burning rate curves of the low-, medium-, and high-density propellants. The high-density propellants are shown with 10% error bars to account for the possible variances in burning rate. The burning rate results from both batches of propellant were combined to form a single burning rate curve for each propellant density group. From this plot, the low-density propellants display a faster burning rate than the medium- and high-density propellants. This trend agrees with previous literature studies that have found that propellants with lower densities tend to have a faster burning rate compared to equivalent propellants with higher densities [12-18]. However, the medium- and high-density propellant burning rate curves are very similar and intersect one another at approximately 1000 psia. This could be an indication that there exists some lower density limit, potentially near 95% TMD, where an increase in burning rate is not observed for propellant densities with 95% < TMD < 100%. However, the burning rates of the low- and medium-density propellants are within the estimated 10% error measurements of the high-density propellants. Thus, an inference about the burning rate behavior of these propellants samples can be made, but it is not certain if it is a true representation of the propellant population for the number of samples tested in this study.

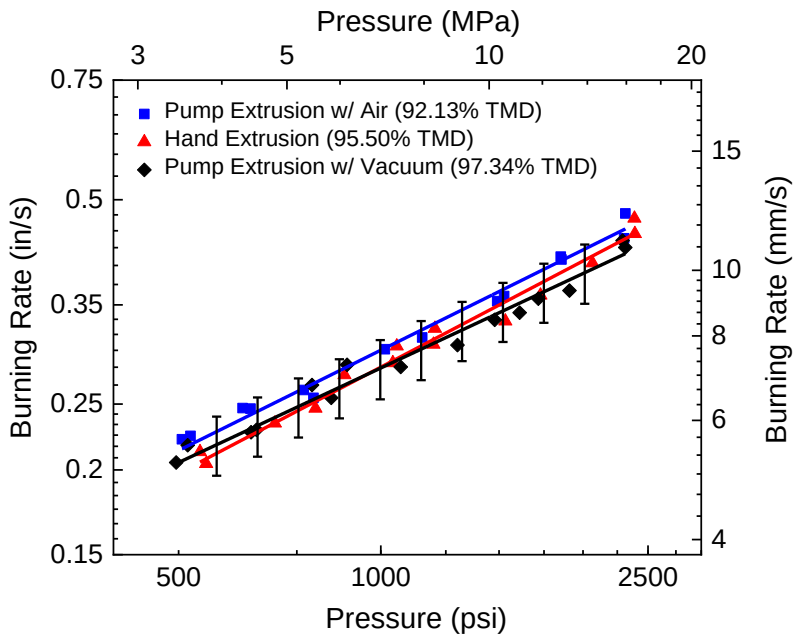

Figure 27. Burning rate plot comparing the low-, medium-, and high-density propellants. The high-density propellants are shown with 10% error bars.

Table 5 compares the burning rate equations and R^2 values of each propellant density group. At 1000 psia, the calculated burning rates of the medium- and high-density propellants are nearly identical at 0.283 and 0.282 in/s, respectively. The low-density propellant was calculated to have a higher burning rate of 0.302 in/s at 1000 psia. This equates to a 6.8% difference in calculated burning rate between the low-density and high-density propellants. Even though the low-density propellant group had the highest R^2 value of 0.985, it does not necessarily indicate that low-density propellants have a lower burning rate variance than medium- or high-density propellants. The low-density propellants had an outlier that was removed from the plot which would have negatively affected its R^2 value. In addition, since only a few propellant samples are burned at each pressure, the R^2 value alone does not provide sufficient information to determine the magnitude of burning rate variance between the low-, medium-, and high-density propellants.

Table 5: Burning rate equations and R^2 values of the low-, medium, and high-density groups for the 75% bimodal propellants.

75% Bimodal Density Group	Burning Rate Equation	Calculated Burning Rate @ 1000 psia (in/s)	R^2 Value
Low Density	$r = 0.0112P^{0.477}$	0.302	0.985
Medium Density	$r = 0.0083P^{0.511}$	0.283	0.978
High Density	$r = 0.0126P^{0.450}$	0.282	0.976

Because of the lack of data in the literature concerning the variance of propellant burning rates, 77% monomodal propellants were manufactured to be burned at two specific pressures rather than a full pressure range. By limiting the testing to two specific pressures, more propellants are able to be tested for burning rates at these points for a stronger statistical analysis. The pressures that were selected were 500 and 3000 psia to better understand how equivalent propellants with different densities will behave at both lower and higher pressures over the range of interest herein. Studying the variance of propellant burning rates is important as it can help indicate the likelihood a rocket motor will perform as designed. If there is a large amount of scatter in the burning rate, the performance of a rocket motor may be more difficult to predict from propellant batch to batch. In addition, the safety of a rocket motor can be negativity impacted if there are large outliers in the burning rate data. If the burning rate is much greater than what was expected at a specific chamber pressure, the rocket motor could be damaged as it may not have been designed to operate at those conditions. Table 6 shows the two different density groups that were tested for the 77% monomodal propellants. These density groups were separated at the 95% TMD mark as the 75% bimodal propellants that were previously tested indicated this point as a possible lower density limit where the burning rate is not significantly affected by a decrease in propellant density.

Table 6: Table comparing the different density groups tested for the 77% monomodal propellants burned at approximately 500 and 3000 psia.

77% Monomodal Density Group	TMD (g/cm^3)	Density Range (g/cm^3)	Density Range (% TMD)
Low Density	1.545	<1.468	<95%
High Density	1.545	≥1.468	≥95%

Over 90 samples of low- and high-density 77% monomodal propellants were tested for burning rates at approximately 500 and 3000 psia. The actual test pressures of the propellants were somewhere between 534 and 584 psia for the low-pressure tests and 3029 and 3160 psia for the high-pressure tests since it is very difficult to test each propellant at the exact same pressures. Even though burning rate increases with pressure, the effect of the difference in burning rate between the actual test pressures is minimal. For example, at the high-pressure tests conducted at approximately 3000 psia, the burning rate difference between the minimum and maximum test pressures was calculated to be 0.004 in/s. However, at the high-pressure tests, the average test pressures of the low- and high-density propellants were 3086 and 3084 psia, respectively, which correlates to a maximum difference in burning rate of 5.70×10^{-5} in/s. Since this difference in burning rate is too small to significantly affect the results of the study, an assumption was made that each propellant was burned at the same pressures for either the low- or high-pressure tests.

Figure 28 displays the box and whisker plot of the low- and high-density propellants tested for burning rate at lower pressures around 500 psia. An outlier can be seen in the high-density propellant group at a burning rate of 0.261 in/s. Even though this point was found to be an outlier in the high-density propellant group, it is still within the burning rate range of the low-density propellants and would not be considered an outlier in the overall sample group. However, this outlier point was removed for the purpose of the statistical analysis. The average burning

rates of the low- and high-density propellants were 0.222 and 0.198 in/s, respectively. From the box and whisker plot, it can be observed that the low-density propellants have a greater variance in burning rate compared to the high-density propellants. The standard deviations of the low- and high-density propellants were 0.029 and 0.011 in/s, respectively. This difference in standard deviation is an indication that low-density propellants can have a less predictable burning rate compared to high-density propellants at lower pressures.

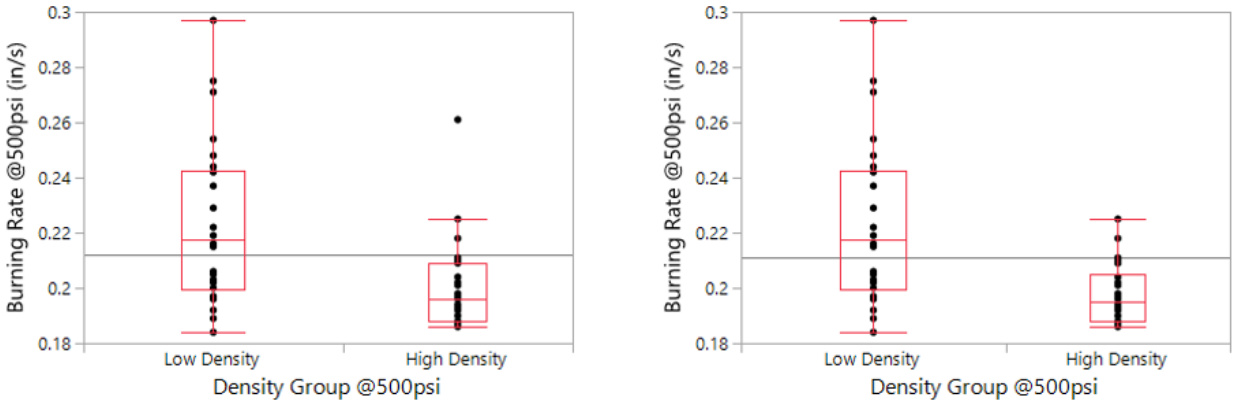

Figure 28. Box and whisker plots of the 77% monomodal burning rate results at approximately 500 psia. The results are shown with an outlier (left) in the high-density propellant group and with the outlier removed (right). The outlier was removed for the purpose of the statistical analysis.

Figure 29 displays the box and whisker plot of the low- and high-density propellants tested for burning rate at higher pressures around 3000 psia. The high-density propellant group had one outlier with a burning rate of 0.438 in/s, while the low-density propellant group had two outliers with burning rates of 0.808 and 0.791 in/s. The high-speed videos captured in these tests were analyzed to verify that these outliers were not the result of the propellant exploding. These outliers were again removed for the purpose of the statistical analysis. The outliers in the low-density propellant group have burning rates that are approximately 153% greater than the overall average burning rate of both propellant density groups. This result is compared to the single

outlier in the high-density propellant that has a burning rate that is approximately 39% greater than the overall average. This trend could be an indication that outliers in propellant burning rates are likely to be more frequent and more extreme in low-density propellants compared to high-density propellants. With these outliers removed, the average burning rates of the low- and high-density propellants are 0.322 and 0.310 in/s, respectively. While the standard deviations of the low- and high-density propellants are 0.041 and 0.012 in/s, respectively. Similar to the low-pressure tests, the low-density propellants are observed to have a greater variance in burning rate compared to high-density propellants at higher pressures.

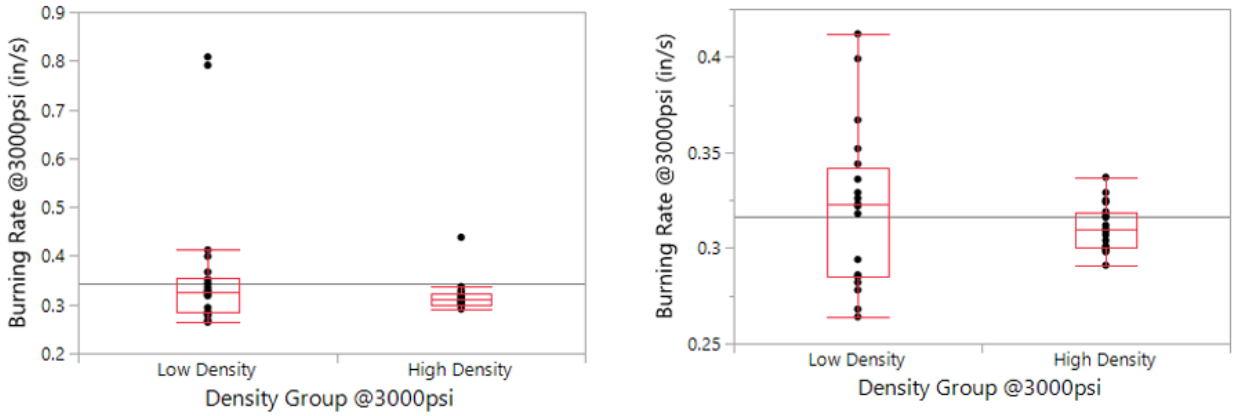

Figure 29. Box and whisker plots of the 77% monomodal burning rate results at approximately 3000 psia. The results are shown with the outliers (left) and with the outlier removed (right). The outliers were removed for the purpose of the statistical analysis.

The results of the statistical analysis of the 77% monomodal propellants burned at approximately 500 and 3000 psia are shown in Table 7. The standard deviation values indicate that low-density propellants will have higher variances in burning rate compared to high-density propellants at both test pressures. The average burning rates of both propellant density groups seem to be consistent with the literature, where propellants with lower densities were found to have higher burning rates than equivalent propellants with higher densities [12-18]. However, most burning rate curves in the literature are formed by testing a few propellant samples at

several different pressures. Even for the 75% bimodal propellants used in this thesis, the burning rate curves were formed by testing only two propellant samples at each pressure point. Since so few propellants are tested at each pressure point, the reliability of the burning rate data can come into question. This is especially true for propellants with low densities as shown by their higher burning rate standard deviation. To determine if the burning rates of the low- and high-density propellants are statistically different, over 90 low- and high-density propellants were burned at approximately 500 and 3000 psia. A Welch's t-test was performed to determine if there is a 95% statistically significant difference between the low- and high-density propellant burning rates. A Welch's t-test is used instead of the traditional Student's t-test because the Welch's t-test is more reliable when comparing groups with unequal sample sizes and/or unequal variances. For the low-pressure tests at approximately 500 psia, the Welch's t-test value was calculated to be 0.0004. Using the standard 95% statistical significance threshold, this means that we can be at least 95% confident that there is a statistically significant difference between the low- and high-density propellant burning rates for the low-pressure tests. For the high-pressure tests at approximately 3000 psia, the Welch's t-test value was calculated to be 0.2246. This means that we cannot be at least 95% confident that the low- and high-density propellants have statistically significant different burning rates for the high-pressure tests. However, we cannot automatically assume that the burning rates between the low- and high-density propellants are the same for the high-pressure tests either. These results seem to indicate that propellant burning rates are more affected at lower pressures by low-density propellants, whereas at higher pressures, propellant burning rates are minimally affected or potentially not affected at all by low-density propellants.

Table 7: Statistical analysis comparing the 77% monomodal low- and high-density propellants at approximately 500 and 3000 psia.

Pressure Group	77% Monomodal Density Group	Average Burning Rate (in/s)	Standard Deviation (in/s)	Welch's t-test
Low Pressure (~500 psia)	Low Density (<95% TMD)	0.222	0.029	0.0004
	High Density (≥95% TMD)	0.198	0.011	
High Pressure (~3000 psia)	Low Density (<95% TMD)	0.322	0.041	0.2246
	High Density (≥95% TMD)	0.310	0.012	

Since the Petersen Research Group historically extrudes composite propellants by hand, a comparison is needed to determine if this extrusion method significantly affects propellant burning rates compared to a high-density mechanical extrusion technique. Figure 30 depicts the box and whisker plots of the 77% monomodal propellants that were hand-extruded compared to the high-density mechanically extruded propellants at approximately 500 and 3000 psia. The hand-extruded propellants had an average propellant density that was 93.06% and 92.72% of the TMD for the low- and high-pressure tests, respectively. These values are lower than the average propellant density of the hand-extruded, 75% bimodal propellants as the monomodal AP distribution, and increase in solids loading (from 75% to 77%) makes it more difficult to tightly pack the propellant manually.

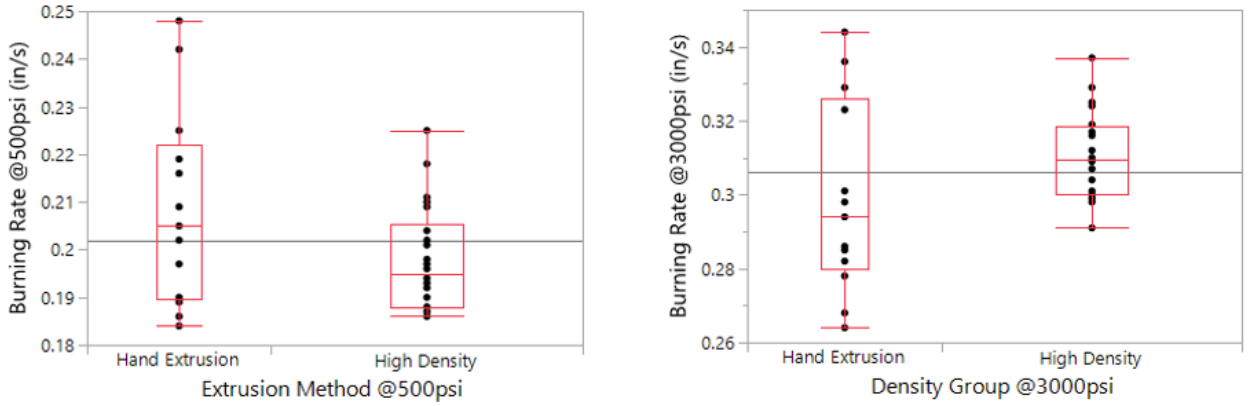

Figure 30. Box and whisker plots of 77% monomodal hand-extruded propellants compared to high-density propellants at approximately 500 (left) and 3000 (right) psia.

The results of the statistical analysis for the hand-extruded and high-density mechanically extruded propellants are shown in Table 8. The standard deviation values indicate that the hand-extruded propellants have a higher burning rate variance than the high-density propellants at both test pressures. The Welch's t-test value was calculated to be 0.1008 and 0.1628 for the low- and high-pressure tests, respectively. However, using a 95% significance threshold, we cannot be certain if the burning rates of the hand-extruded propellants are actually statistically significantly different than the burning rates of the high-density propellants for both the low- and high-pressure tests. Nonetheless, we cannot automatically assume that the propellant burning rates are the same either. These results seem to indicate that the hand-extruded propellants are able to provide comparable burning rate results to the high-density mechanically extruded propellants within the statistical variation of obtaining the burning rate from such samples.

Table 8: Statistical analysis comparing the 77% monomodal hand-extruded and high-density propellants at approximately 500 and 3000 psia.

Pressure Group	77% Monomodal Propellant Group	Average Burning Rate (in/s)	Standard Deviation (in/s)	Welch's t-test
Low Pressure (~500 psia)	Hand Extrusion (93.06% TMD)	0.209	0.021	0.1008
	High Density (≥95% TMD)	0.198	0.011	
High Pressure (~3000 psia)	Hand Extrusion (92.72% TMD)	0.299	0.026	0.1628
	High Density (≥95% TMD)	0.310	0.012	

Data Processing and Uncertainty

When determining the densities and burning rates of propellants, there will be a certain degree of uncertainty associated with the accuracy of the measurements. The measurement uncertainties were estimated using the root-sum-square (RSS) method for the caliper method of determining propellant density, Archimedes' method of determining propellant density, and propellant burning rate.

The uncertainty of the Omega PX359-7.5KG5V used to determine chamber pressure is reported by the manufacturer to be 0.25%. This correlates to an estimated uncertainty of 500 ± 1.25 psia at the low-pressure tests and 3000 ± 7.50 psia at the high-pressure tests.

The caliper method of determining propellant density involves using a digital caliper with a resolution of 0.0005 in. and a scale with a resolution of 0.01 g. The propellant is cured in a piece of Teflon® tubing with an inner diameter of 0.1875 in. However, uncertainties associated with human errors during measurement of the propellant length using the digital calipers was estimated to be 0.0050 in. It is important to note that the actual measurement error will change each time a measurement is taken due to the nature of human error. In addition, during the early stages of curing, propellant material can trickle out the side of the Teflon® tubing due to the liquid nature of the propellant slurry. This leakage can result in a reduction of the propellant diameter, which is why the diameter is ultimately verified using the digital calipers. The associated uncertainty of the propellant sample diameter is estimated to be 0.0025 in. A randomly selected propellant sample with a mass of 0.69 g, length of 0.9965 in, and diameter of 0.1875 in was used to estimate the total uncertainty. Using the RSS method, the total uncertainty associated with the caliper method of determining the density of the randomly selected propellant sample was estimated to be 1.530 ± 0.47 g/cm^3 or ± 3.08%.

The Archimedes' method of determining propellant density relies primarily on using a scale with a 0.01 g resolution. However, the density of the HTPB medium in which the propellant is suspended within is also needed to determine the propellant density. Since the manufacturer did not report an uncertainty value for the HTPB density, it was estimated to be 0.001 g/cm^3 to account for potential changes in HTPB density due to impurities and temperature fluctuations. The same randomly selected propellant that was previously mentioned was used again to estimate the total uncertainty. Using the RSS method, the total uncertainty associated with the Archimedes' method of determining the density of the randomly selected propellant sample was estimated to be 1.516 ± 0.043 g/cm^3, or ± 2.84%. Even though the estimated total uncertainty of the Archimedes' and caliper methods are comparable, the Archimedes' method was selected as the method of choice as there are fewer human errors associated with its propellant density measurement. The reduced likelihood of human error associated with the Archimedes' method allows it to provide more consistent measurements of propellant density.

Burning rate plots are commonly shown with 10% error bars to account for the variances in burning rate. This practice is a fairly adequate error estimation based on the burning rate results of the 77% monomodal propellants with high densities. The associated burning rate error bars were calculated to be approximately 11.1% and 7.7% at low and high pressures, respectively. These error bars were determined by dividing the mean burning rate by the burning rate standard deviation. The RSS method was also used to estimate the total burning rate uncertainty for the associated propellant length and burn time measurements. The total burning rate uncertainty at lower pressures around 500 psia and higher pressures around 3000 psia was estimated to be ±5.58% and ±2.82%, respectively.

CHAPTER VI

SUMMARY

Low propellant density caused by voids can have significant effects on the performance and safety of composite solid propellants. From the literature, low-density propellants are often found to have an inflated burning rate compared to equivalent propellants with higher densities [12-18]. An experiment was designed to better control and study the effects of propellant density (in terms of TMD) on burning rate. A custom extrusion system was designed and optimized to be able to produce low- and high-density propellants. Low-density propellants were created by deliberately introducing air into the system to propagate void formation. High-density propellants were manufactured by attaching the extruder to a vacuum to remove as much air as possible to mitigate the formation of voids. A more precise and accurate way of measuring propellant density based on Archimedes' principle was also designed to mitigate human error.

A burning rate curve between 500 and 2500 psia was developed for the 75% bimodal propellants with low, medium, and high densities. The low-density propellants with an average density of 92.13% TMD displayed burning rates that were higher than the medium- and high-density propellants that had an average density of 95.50% and 97.34% TMD, respectively. However, the burning rate curve of the low-density propellants was within the 10% error bars of the high-density propellants. Thus, an inference can be made on the burning rate behavior of low-density propellants, but it is not certain if it is a true representation of the population.

To better understand the burning behavior of propellants with differing densities, 77% monomodal propellants were burned at two specific pressures rather than a full range of pressures. In this scenario, low-density propellants were categorized as propellants with densities less than 95% TMD, whereas high-density propellants had densities greater than or equal to 95%

TMD. Both propellant density groups were burned at low and high pressures around 500 and 3000 psia, respectively. At both low and high pressures, the low-density propellants had a greater burning rate standard deviation than the high-density propellants. This larger deviation indicates that low-density propellants are more likely to exhibit greater variances in burning rate than high-density propellants. A Welch's t-test was used to determine if there is a statistically significant difference between the burning rate of the two propellant density groups. At low pressures, it was determined with at least 95% confidence that there is indeed a statistically significant difference between the burning rates of the low- and high-density propellants. However, at high pressures, we cannot be 95% confident that there is a statistically significant difference between the burning rate of the low- and high-density propellants. The low-density propellants were also shown to have more frequent and more extreme outliers in burning rate which can also affect the overall safety of a rocket.

REFERENCES

[1] Galfetti, Luciano & F., Severini & DeLuca, Luigi & Marra, Gianluigi & Meda, Laura & R., Braglia. (2004). Ballistics and Condensed Residues of Aluminized Solid Rocket Propellants.

[2] Singh, Gurdip & Sengupta, S. & a, I. & a, Shalini & a, Reena & a, Supriya. (2013). Nanoparticles of Transition Metals as Accelerants in the Thermal Decomposition of Ammonium Perchlorate, Part 62. Journal of Energetic Materials. 31. 165–177. 10.1080/07370652.2012.656181.

[3] SureshBabu, K.V. & KanakaRaju, P. & Thomas, C.R. & SyedHamed, A. & Ninan, K.. (2017). Studies on composite solid propellant with tri-modal ammonium perchlorate containing an ultrafine fraction. Defence Technology. 13. 10.1016/j.dt.2017.06.001.

[4] Ke-Xi, Y., Ze-Ming, T. and Guo-Juan, W. (1986), Viscosity Prediction of Composite Solid Propellant Slurry. Propellants, Explosives, Pyrotechnics, 11: 167-169. https://doi.org/10.1002/prep.19860110603

[5] Yaman, Hayri & Çelik, Veli & Değirmenci, Ercan. (2014). Experimental investigation of the factors affecting the burning rate of solid rocket propellants. Fuel. 115. 794-803. 10.1016/j.fuel.2013.05.033.

[6] Dillier, Catherine Anne Marie (2021). High-Pressure Exponent Break of AP/HTPB-Composite Propellants. Doctoral dissertation, Texas A&M University.

[7] Petersen, Eric & Thomas, James & Dillier, Catherine. (2019). High-Pressure Propellant Burning Rate Measurements at Texas A&M University.

[8] Thiyyarkandy, Bejoy & Jain, Mukesh & Dombe, Ganesh & Maurya, Mehilal & Singh, Praveen & Bhattacharya, Bikash. (2012). Numerical Studies on Flow Behavior of Composite Propellant Slurry During Vacuum Casting. Journal of Aerospace Technology and Management. 4. 197-203. 10.5028/jatm.2012.04021212.

[9] Adde, Yeshurun (Kibret) & Alemayehu, & Lulseged, G & Adde, Y & Alemayehu, Lulseged & Solomon, Gedlu. (2020). Design of a Solid Rocket Propulsion System. International Journal of Aeronautical Science & Aerospace Research. 224-229. 10.19070/2470-4415-2000027.

[10] R., Afni & Hajar Abdillah, Luthfia & Ardianingsih, Retno & Sitompul, Hamonangan & Budi, Rika & Hartaya, Kendra & Wibowo, Heri. (2021). Thixotropic Behavior in Defining Particle Packing Density of Highly Filled AP/HTPB-Based Propellant. Symmetry. 13. 1767. 10.3390/sym13101767.

[11] Srihakulung, Ornin. (2012). Quality control of Solid Propellant casting process by using X-ray technique.

[12] Verma, Sumit & Periyapatna, Ramakrishna. (2014). Dependence of density and burning rate of composite solid propellant on mixer size. Acta Astronautica. 93. 130-137. 10.1016/j.actaastro.2013.07.016.

[13] Ponti, Fabrizio & Mini, Stefano & Fadigati, L. & Ravaglioli, Vittorio & Annovazzi, Adriano & Garreffa, V.. (2021). Effects of inclusions on the performance of a solid rocket motor. Acta Astronautica. 189. 10.1016/j.actaastro.2021.08.030.

[14] Toft, Hans Olaf. Voids in Solid Propellants. DANSK AMATØR RAKET KLUB, 2002.

[15] Foltran, Antonio & Moro, Diego & Dicati Pereira da Silva, Nicholas & Ferreira, Ana & Araki, Luciano & Marchi, Carlos. (2015). Burning Rate Measurement of KNSu Propellant Obtained by Mechanical Press. Journal of Aerospace Technology and Management. 7. 193-199. 10.5028/jatm.v7i2.431.

[16] McClain, Monique & Gunduz, I. & Son, Steven. (2018). Additive manufacturing of ammonium perchlorate composite propellant with high solids loadings. Proceedings of the Combustion Institute. 37. 10.1016/j.proci.2018.05.052.

[17] Mathesius, Kelly & Hansman, R.. (2019). Manufacturing Methods for a Solid Rocket Motor Propelling a Small, Fast Flight Vehicle.

[18] Kohga, Makoto. (2008). Effect of Voids inside AP Particles on Burning Rate of AP/HTPB Composite Propellant. Propellants Explosives Pyrotechnics - PROPELLANT EXPLOS PYROTECH. 33. 249-254. 10.1002/prep.200700234.

[19] Beckstead, Merrill & Derr, R. & Price, C.. (1970). A Model of Composite Solid-Propellant Combustion Based on Multiple Flames. AIAA Journal. 8. 2200-2207. 10.2514/3.6087.

[20] Missile Technology Control Regime Annex Handbook. (1996). Federation of American Scientists.

[21] Demko, Andrew R. (2013). Tailoring Composite Solid Propellants to Produce a Plateau Burning Profile. Master's thesis, Texas A&M University.

[22] Alain Davenas. (1993). Solid Rocket Propulsion Technology. Pergamon Press, Tarytown, New York.

[23] Terry McCreary. (2014). Experimental Composite Propellant. Murray, Kentucky.

[24] Stephens, M., Sammet, T., Carro, R., LePage, A., Petersen, E. (2012). “Comparison of Hand and Mechanically Mixed AP/HTPB Solid Composite Propellants,” 43rd AIAA/ASME/SAE/ASEE Joint Propulsion Conference & Exhibit, Vol. 8, No. 11, Cincinnati, OH.

[25] Sutton, George P., and Oscar Biblarz. (2001). Rocket Propulsion Elements. John Wiley & Sons.

[26] GODAI, T. (1970). “Flame Propagation into the Crack of Solid- Propellant Grain.” AIAA Journal, vol. 8, no. 7, pp. 1322–1327., https://doi.org/10.2514/3.5892.

[27] Kumar, Mridul, et al. (1981). “Flame Propagation and Combustion Processes in Solid Propellant Cracks.” AIAA Journal, vol. 19, no. 5, pp. 610–618., https://doi.org/10.2514/3.50983.

[28] Aravind, M., Jerin, J., Rariprasad., V., Ganesh, B.K., Aswin, C. and Kumar, V.R.S. (2013). “In-house Manufacture of Variable Burning Rate Propellant Bangles for Nozzleless Propulsion”, Proceedings of the International Conference on Aerospace, Mechanical, Automotive and Materials Engineering, Paris, France.

[29] Nakka, R.A. (1984). “Solid Propellant Rocket Motor Design and Testing”, Bachelor of Science Thesis, University of Manitoba, Manitoba, Canada

[30] Vyverman, T. (1978), “The Potassium Nitrate — Sugar Propellant”, Report, Belgium.

[31] Gross, Matthew & Beckstead, Merrill. (2010). Diffusion flame calculations for composite propellants predicting particle-size effects. Combustion and Flame. 157. 864-873. 10.1016/j.combustflame.2009.09.004.

[32] Thomas, James & Morrow, Gordon & Dillier, Catherine & Petersen, Eric. (2019). Comprehensive Study of Ammonium Perchlorate Particle Size/Concentration Effects on Propellant Combustion. Journal of Propulsion and Power. 36. 1-6. 10.2514/1.B37485.

[33] Dillier, Catherine & Demko, Andrew & Stahl, Jacob & Reid, David & Petersen, Eric. (2017). Temperature Sensitivity of AP/HTPB-Based Rocket Propellants Using a New High-Pressure Strand Burner. 10.2514/6.2017-0830.